IEEE Journal of Microwaves

Received 6 October 2022; revised 16 December 2022 and 28 February 2023; accepted 3 March 2023.
Date of current version 7 April 2023.

Digital Object Identifier 10.1109/JMW.2023.3255581

RF Energy Harvesting and Wireless Power Transfer for Energy Autonomous Wireless Devices and RFIDs

KYRIAKI NIOTAKI [1] (Member, IEEE), NUNO BORGES CARVALHO [2] (Fellow, IEEE), APOSTOLOS GEORGIADIS [3] (Fellow, IEEE), XIAOQIANG GU [4,5] (Member, IEEE), SIMON HEMOUR [6] (Senior Member, IEEE), KE WU [5] (Fellow, IEEE), DIOGO MATOS [2,14] (Graduate Student Member, IEEE), DANIEL BELO [7], RICARDO PEREIRA [2], RICARDO FIGUEIREDO [2] (Member, IEEE), HENRIQUE CHAVES [2], BERNARDO MENDES [2], RICARDO CORREIA [2] (Member, IEEE), ARNALDO OLIVEIRA [2] (Member, IEEE), VALENTINA PALAZZI [8] (Member, IEEE), FEDERICO ALIMENTI [8] (Senior Member, IEEE), PAOLO MEZZANOTTE [8] (Member, IEEE), LUCA ROSELLI [8] (Fellow, IEEE), FRANCESCA BENASSI [9] (Member, IEEE), ALESSANDRA COSTANZO [9] (Fellow, IEEE), DIEGO MASOTTI [9] (Senior Member, IEEE), GIACOMO PAOLINI [9] (Member, IEEE), ALINE EID [10] (Member, IEEE), JIMMY HESTER [11] (Member, IEEE), MANOS M. TENTZERIS [12] (Fellow, IEEE), AND NAOKI SHINOHARA [13] (Senior Member, IEEE)

(Invited Paper)

[1]LTCI, Télécom Paris, Institut Polytechnique de Paris, 91120 Palaiseau, France
[2]Instituto de Telecomunicações, Universidade de Aveiro, 3810-193 Aveiro, Portugal
[3]2582 CN The Hague, The Netherlands
[4]Department of Electrical and Computer Engineering, McGill University, Montreal, QC H3A 0E9, Canada
[5]Poly-GRAMES Research Center, Polytechnique Montreal, Montreal, QC H3T 1J4, Canada
[6]IMS Laboratory, CNRS UMR 5218, Bordeaux INP, University of Bordeaux, 33045 Talence, France
[7]Huawei Technologies Sweden AB, 16494 Kista, Sweden
[8]Department of Engineering, University of Perugia, I-06125 Perugia, Italy
[9]DEI "Guglielmo Marconi", University of Bologna, 40136 Bologna, Italy
[10]Department of Electrical Engineering and Computer Science, University of Michigan Ann Arbor, Ann Arbor, MI 48109 USA
[11]Atheraxon, Inc., Atlanta, GA 30308 USA
[12]School of Electrical and Computer Engineering, Georgia Institute of Technology, Atlanta, GA 30332-0250 USA
[13]Research Institute for Sustainable Humanosphere, Kyoto University, Kyoto 606-8501, Japan
[14]Sinuta S.A., 3860-529 Estarreja, Portugal

CORRESPONDING AUTHOR: Kyriaki Niotaki (e-mail: kyriaki.niotaki@telecom-paris.fr).

ABSTRACT Radio frequency (RF) energy harvesting and wireless power transmission (WPT) technologies —both near-field and far-field—have attracted significant interest for wireless applications and RFID systems. We already utilize near-field WPT products in our life and it is expected that RF EH and far-field WPT systems can drive the future low-power wireless systems. In this article, we initially present a brief historical overview of these technologies. The main technical challenges of rectennas and WPT transmitters are discussed. Furthermore, this paper presents the recent advances on the development of these technologies, including the possibility of powering RFID systems through the millimeter wave power from 5G networks, the trends in flexible rectennas design and the technological developments on the simultaneous wireless information and power transfer (SWIPT).

INDEX TERMS Backscatter, wireless communications, electromagnetic harvesting, RF energy harvesting, IoT, wireless power transfer, energy harvesting, rectenna, antenna array, millimeter-wave, flexible rectennas, simultaneous wireless information and power transfer, MTT 70th Anniversary Special Issue.

I. INTRODUCTION

The exponential growth of low-power wirelessly connected devices (estimated 40 billion devices by 2025 [1]) brings significant energy challenges for their autonomous operation. Batteries usage is challenging for a plethora of environmental, economical and practical reasons. Alternative energy sources - both intentional and unintentional - can complement or replace batteries usage.

To overcome the dependency on batteries, ambient energy can be collected, converted and finally utilized; this is known as energy harvesting (EH) or energy scavenging. Solar, thermal, kinetic and Radio Frequency (RF) sources are potential solutions for the energy autonomous operation of the Internet of Things (IoTs) and machine-to-machine devices [2], [3].

RF energy harvesting (RF EH) refers to the concept of scavenging the otherwise wasted energy that is not utilized by the end users [4]. This implies that the energy sources are existing and opportunistic; examples of such sources are TV broadcast and wireless networks. An alternative solution towards the autonomous operation of these emerging technologies is the intentional power transfer towards the targeted application. Wireless Power Transmission (WPT) can be near-field or far-field [2], [5], [6], [7]. The increased interest for RF EH and WPT technologies has resulted in a number of research and development activities on these areas, e.g. [8], [9].

In this article, we present the recent advances of RF EH and WPT technologies along with future research directions. We initially present a brief history on the development of these technologies, starting from Maxwell's equations up to present (Section II). To assess the feasibility of RF EH, firstly we need to understand the available power levels in the environment [10], [11], [12], [13], [14], [15]. Section III summarizes a series of ambient RF power measurement campaigns that have been made worldwide and highlights the bands with higher power density in cities and suburban areas. Despite the low-power ambient RF availability, the emergence of ultra low-power modern devices and applications make nowadays RF EH technology an attractive solution [16], [17], [18], [19].

The rectification efficiency of the energy harvester is a critical parameter for the design of efficient RF EH systems. Section IV discusses the challenges of designing high performance rectifiers and reviews the state-of-the-art rectification efficiency versus input power and operating frequency. It also highlights some important research directions on improving rectifier performance outlining diode modeling and technologies. Furthermore, novel rectennas designs based on flexible materials are discussed in Section V. In the case of WPT systems, dedicated power sources with high power and beamforming capabilities can result in higher RF power density levels adjusted for various purposes [20]. Section VI focuses on the transmitter side of a far-field WPT system.

As more and more cities deploy 5G infrastructure, the possibility of utilizing the mid-band 5G and millimeter wave (mm-wave) frequencies for the aforementioned technologies needs to be considered and deeply investigated. Section VII focuses on the 5G mm-wave power availability and properties, and presents the new prospect of utilizing 5G millimeter wave power for Radio Frequency Identification (RFID) systems.

The combination of electromagnetic energy sources with communication signals has triggered the research interest recently. In this last decade, techniques for simultaneous wireless information and power transfer (SWIPT) have been widely addressed in the RFID field and beyond [21], [22]. Simultaneous wireless powering and data communication can be achieved with transceivers operations in the near reactive field at low (30–300 kHz) and high (3–30 MHz) frequencies or in the far radiative field, exploiting microwaves (300 MHz–30 GHz) and millimeter waves (30–300 GHz).

Near-field (NF) SWIPT implies mutual reactive magnetic or electric coupling, depending on the fact that inductive coils or capacitive electrodes are exploited for power and data exchange, respectively. Typically, power levels for power transmission cover the range from few W to kW, whereas for data transfer lower levels (μW to mW) are involved. In the far-field (FF) SWIPT the energy sources are further from the targeted application. Section VIII provides an overview of the recent SWIPT developments, including both near-field and far-field systems.

In summary, the structure of this article is as follows. Section II presents a brief historical overview for RF EH and WPT technologies. Section III focus on the available ambient power levels for RF energy harvesting applications, while Section IV is dedicated on the rectification efficiency of RF EH systems with an emphasis on diode modeling and technologies. Section V focuses on flexible rectennas and Section VI discusses the transmitter side of a far-field WPT system. Section VII discusses the new prospect of utilizing 5G millimeter wave power to power RFID systems, while Section VIII presents the recent advances in SWIPT technologies. Finally, Section IX concludes this article.

II. HISTORICAL OVERVIEW OF WPT AND RF EH TECHNOLOGIES

In this section a brief history on the evolution of wireless power transmission and RF energy harvesting is presented. The works [20], [23], [24], [25], [26], [27], [28], [29], [30], [31], [32] represent a non-exhaustive list of publications that provide a more detailed description of the historical events. A careful analysis of the research in the recent years is also explored, with a focus on more recent advances. Fig. 1 summarizes graphically some major steps in the development of RF EH and wireless power transmission, starting from Maxwell's equations up to recent experimental demonstrations.

In 1864, James C. Maxwell predicted the radio waves as an energy form. Two decades later, Heinrich Hertz experimentally verified Maxwell's theory by transmitting and receiving radio waves. Following the work of Maxwell and Hertz, Guglielmo Marconi publicly transmitted wireless signals at the end of the 19th century. Nicola Tesla strongly experimented with WPT; he performed the first WPT trial

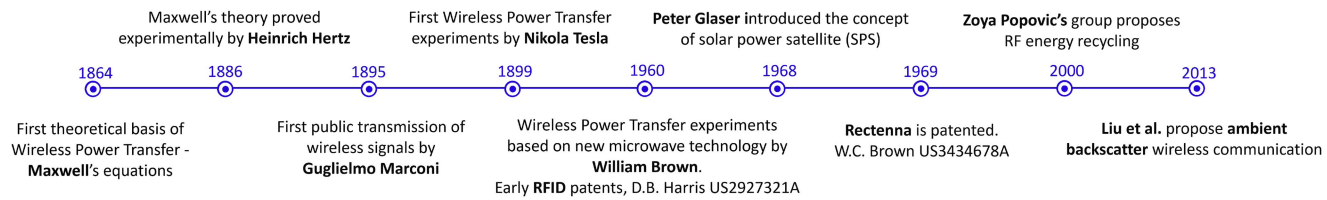

FIGURE 1. Major milestones of the evolution of RF energy harvesting and wireless power transfer technology from Maxwell's equations up to more recent times.

and his work focused on both near-field and far-field wireles power trasmission. After Tesla's experiments, wireless power transfer was not investigated much due to the unavailability of the required technology for high power generation.

However, the recent technological advancements enabled a wide range of far-field WPT experiments [23], [33]. In 1960 s, William Brown created the first rectifying antenna (rectenna). In 1964, William Brown conducted the first experiment of wireless power transfer to a drone. The idea of solar space satellite (SPS) was introduced later in 1968. In this concept, solar energy can be scavenged and transmitted to earth. The received energy can be then collected and converted to dc using rectennas.

In last decades, WPT and RF EH technologies have been developed and many experiments and demonstrations have taken place worldwide. As an example, Fig. 2 shows the experiment MILAX (MIcrowave Lifted Airplane eXperiment) which took place in Japan in 1992 [25], [32]. Fig. 2(a) and (b) illustrate a photo of the wirelessly powered airplane experiment and a closer look to the WPT system elements, respectively. The transmitter is placed on the top of the car and the rectenna is integrated on the airplane. Finally, Fig. 2(c) shows the phased-antenna array placed on the top of the car.

These technologies have been explored and further developed from companies. Near-field WPT technologies are more mature from a commercial point of view [34]; e.g. wireless charging of everyday devices, such as cellphones and toothbrushes. A few examples of companies that work on the development of far-field WPT systems are Ossia, PowerCast, Energous, Wi-charge and TechNovator [35]. Information about the ongoing development of regulatory frameworks and standards can be found in [35], [36].

Finally, among the milestones related to RF energy harvesting, while many commercial applications focus on wirelessly powering devices using intentional radiators to provide the desired RF power, an exciting possibility is the concept of recycling ambient RF energy from existing RF sources that unintentionally transmit signals, or rather do not explicitly transmit RF signals for the purpose of RF powering, as originally proposed by the group of Prof. Z. Popovic at the University of Colorado, Boulder [26]. Furthermore, researchers from Univ. of Washington proposed the concept of ambient backscatter wireless communication [27], combining the ideas of RF energy recycling and communication utilizing existing ambient RF signals. In [37] the authors showed for the first time a trully indoor solution for WPT charging of indoor devices, and achieve a TRL of 4 in this experiment.

TABLE 1. Selected Surveys on Ambient RF Energy Density

City year	DTV	LTE/GSM 700/850/900	LTE/GSM 1700/1900	Wi-Fi
Kyoto 2012 [39]	−38 dBm	−25 dBm	-	-
London 2013 [14]	−60.5 dBm/cm^2	−44.4 dBm/cm^2	−40.7 dBm/cm^2	−67.4 dBm/cm^2
Boston* 2018 [40]	3%	−11.1dBm 92%	5%	-
Montreal** 2019 [41]	−68.45 dBm/cm^2	−55.18 dBm/cm^2	−52.14 dBm/cm^2	−77.42 dBm/cm^2

*Measurement was finished in 2016. Results are percentage times that this band contains the highest RF energy among all frequency bands.
**Results are average ambient RF power density in the downtown area.

III. ENERGY SPECTRAL DENSITY

One vital research direction of energy harvesting lies in scavenging ambient radio frequency (RF) energy from our living environment. In cities, ambient RF energy is pervasive, which comes from digital TV (DTV) towers, cellular communication networks, and Wi-Fi hotspots. DTV signals usually are below 800 MHz, and Wi-Fi signals are at either 2.4 GHz or 5 GHz. A significant portion of ambient RF energy origins from cellular base stations. As shown in Fig. 3, existing cellular networks of 4G and before offer ambient RF energy below 2.7 GHz. While more and more cities are deploying 5G infrastructure, people are observing ambient RF energy in sub-6 GHz and millimeter wave (mm-wave) 5G bands [38].

A critical reference for building energy autonomous wireless devices based on ambient RF energy recycling is understanding how much such energy is available in our environment. Since more than a decade ago, researchers around the world have been doing surveys on RF spectral density along with the rapid development of cellular network technologies. Table 1 has summarized the measurement results of ambient RF energy density with at least 20 testing points. Since all these measurements were finished before a large deployment of 5G, results only cover DTV, Wi-Fi, and cellular communication bands (4G and before). Table 1 shows that ambient RF energy in the LTE frequency bands has the highest

(a)

(b)

(c)

FIGURE 2. (a) Experiment of wirelessly powered airplane in Japan in 1992, (b) transmitter installed on the top of the car and rectenna integrated with the airplane, and (c) close look on the phased-antenna array [32].

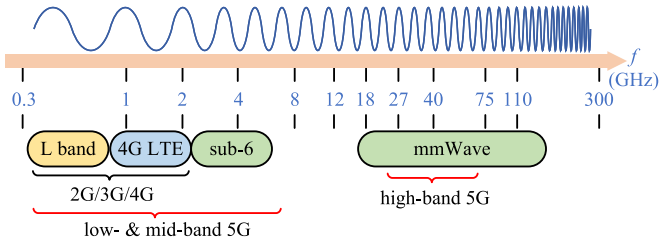

FIGURE 3. A significant portion of ambient RF energy comes from the existing 2G/3G/4G and expanding 5G networks. With a speedy rollout of 5G worldwide, ambient RF energy at higher frequency bands is/will soon be in place.

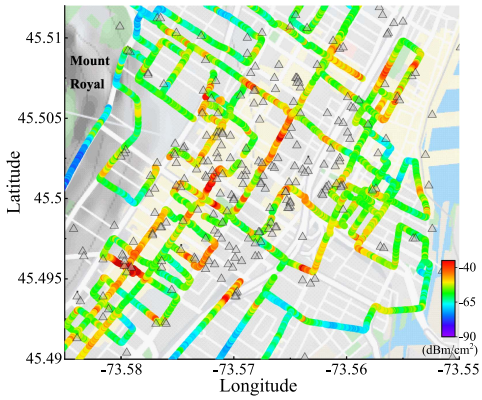

(a)

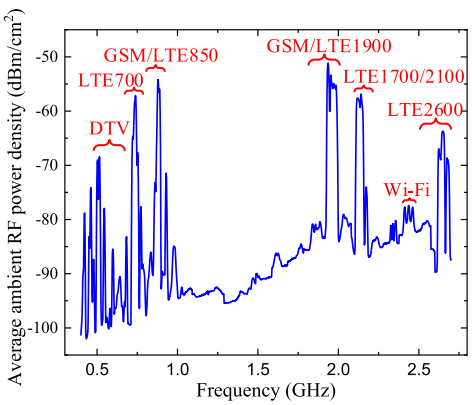

(b)

FIGURE 4. (a) Ambient RF power density of GSM/LTE 1900 band in downtown Montreal [41]. The triangle symbol marks the cellular base station and (b) average ambient RF power density in downtown Montreal across a frequency band from 400 MHz to 2.7 GHz [41].

power density compared to the DTV and Wi-Fi frequency bands [14], [39], [40], [41]. And such an observation is consistent across multiple cities in the world, which indicates that energy harvesting in a populated area should target cellular communication bands.

To assess the feasibility of energy autonomous wireless devices based on harvesting ambient RF energy in cities, a large-scale RF survey was conducted in Montreal [41]. Fig. 4(a) demonstrates the ambient RF power density of the GSM/LTE 1900 band in the downtown area, which is the band with the highest power density among all bands, as shown in Fig. 4(b). The power density is highly dependent on the distribution of cellular base stations based on Fig. 4(b). The highest power density obtained is about -26 dBm·cm^{-2}. Besides GSM/LTE1900 band, other cellular communication

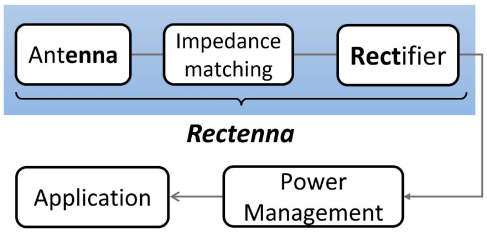

FIGURE 5. Block diagram of RF energy harvester, with rectifying antenna (rectenna) highlighted in blue.

bands, including LTE700, GSM/LTE850, and LTE1700/2100, have a power density larger than -60 dBm·cm^{-2}.

Compared to downtown areas equipped with more cellular base stations, suburban areas usually would see a dramatic drop in RF power density in cellular communication bands. Advantages of harvesting DTV signals include good availability as DTV signals are less dependent on human activities and enhanced conversion efficiency due to the operation in typically lower frequency bands than other communication systems.

Based on RF surveys conducted in various cities, feasible ambient energy harvesting applications shall target a power density lower than -25 dBm·cm^{-2}. Also, as 5G networks are being quickly deployed, RF surveys should be updated regularly. In particular, future RF surveys need to cover new frequency bands, including mid-band 5G and high-band/mm-wave 5G. Mid-band 5G extends the cellular frequency band to 6 GHz, serving metropolitan areas. High-band 5G adopts new mm-wave frequency bands, mainly focusing on dense urban areas.

Furthermore, besides ambient RF energy associated with low power density, wireless power transmission can be implemented through dedicated power sources with higher power and beamforming technology [20]. In this case, RF power density can be well-controlled or adjusted for different purposes. Hybrid approaches of collecting energy from both a dedicated energy source and existing sources can be also considered [42].

IV. ENERGY HARVESTER, DIODE MODELING, AND TECHNOLOGIES

The rectifying antenna, or rectenna for short, is the most critical component for the performance of an RF energy harvester. A simplified block diagram of the key components of an energy harvester is shown in Fig. 5. The works [43], [44], [45], [46], [47], [48] analyze further its structure. Nonlinearity does the trick of frequency conversion, converting RF input signals into higher harmonics and direct current (dc). Various applications have their own desired output. Energy harvesting application maximizes dc output by minimizing the energy conversion to other harmonics ranks to enhance the conversion efficiency [49]. Any nonlinear device can distribute a Continuous Wave (CW) signal over its harmonics. Typical nonlinear devices are diodes and transistors. Energy

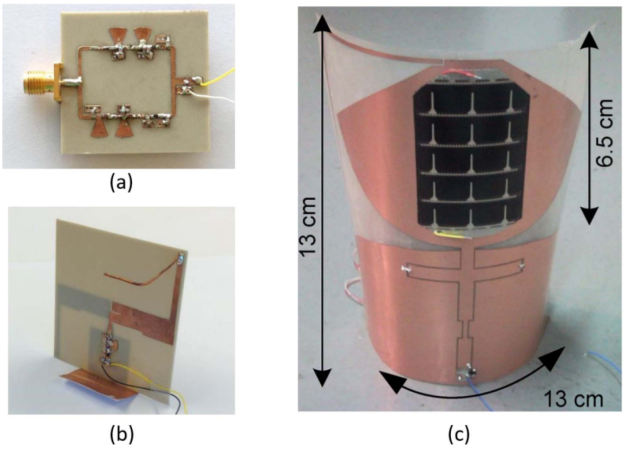

FIGURE 6. (a) Rectifier based on resistance compression network, (b) rectifying antenna (rectenna), and (c) hybrid solar-electromagentic energy harvester. After [52], [55], [56].

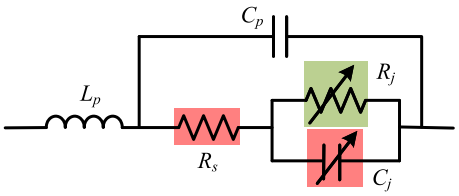

FIGURE 7. A Shockley diode model can be used to model Schottky diodes. In the RF energy harvesting application, the nonlinear junction resistance R_j, highlighted in green, provides dc power and the nonlinear junction capacitance C_j together with the series resistance R_s in red dissipate dc power. L_p and C_p represent the diode package parasitic inductance and capacitance respectively.

harvesting, especially in a low-power range, requires zero-bias operation (energy is too sparse to be wasted in biasing).

Moreover, the impedance of the device should be "matchable" to the energy-capturing antenna, which can be derived from a low zero-bias junction resistance (typically no larger than a few kΩ). As a result, Schottky diodes, whose junction potential is about 0.15 to 0.45 V, are widely used in RF energy rectifier design. A comprehensive survey of rectifier circuits using different types of diode devices including integrated circuits utilizing diode connected transistor devices is presented in [50].

Some recent works match directly the antenna and the rectifier omitting the impedance matching (IM) network [47], [51], while novel impedance matching networks, e.g. resistance compression networks (RCN), have been proposed to improve rectifiers performance by reducing its sensitivity to environmental conditions changes [52], [53], [54]. Fig. 6(a) and (b) show a rectifier based on RCN networks and a rectenna, respectively [52], [55].

A Schottky diode can be characterized by the Shockley diode model, as shown in Fig. 7. It contains nonlinear junction resistance R_j, nonlinear junction capacitance C_j, series resistance R_s, and packaging parasitics C_p and L_p.

When used in rectifier design, the nonlinear junction resistance R_j can be seen as an RF-current-controlled dc source. At

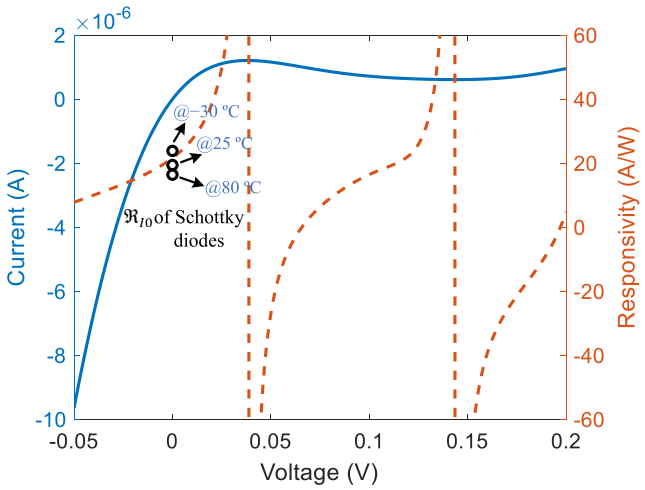

FIGURE 8. I-V curve of a backward tunnel diode and its current responsivity [61]. Physical limits of Schottky diode's R_{I0} at three temperatures are also marked.

high frequencies, the impedance of the junction capacitance C_j gets lower than R_j and draws more RF current, which results in lower RF current being converted by the nonlinear junction resistance. Hence, both C_j and R_s impede the rectifying operation and should be chosen as low as possible. Based on the understanding mentioned above and the Shockley diode model, an analytical model can be derived for rectification efficiency prediction [57], [4]. The current generated by nonlinear junction resistance I_{diode} due to RF input power can be expressed by:

$$I_{diode} = I_s \left(e^{\frac{V_{on}}{nV_t}} - 1 \right) \tag{1}$$

in which I_s, V_{on}, n, and V_t are diode saturation current, voltage magnitude across the junction, diode ideality factor, and thermal voltage, respectively. Since I_{diode} contains all frequency components of current, including fundamental signal, dc, and harmonics, RF input P_{in} and dc output P_{dc} can be obtained based on I_{diode} [49]. Thus, rectification efficiency can be calculated:

$$\eta = \frac{P_{dc}}{P_{in}} \times 100\% \tag{2}$$

A more general way to estimate the nonlinearity of any kind of diode is to use current responsivity R_I, which is defined as the ratio of dc output current over the RF input, and its unit is [A/W] [58], [59]. It can also be computed from the first and second derivatives of diode's I–V curve [60]:

$$R_I = \frac{1}{2} \frac{\frac{d^2 I}{d^2 V}}{\frac{dI}{dV}} \tag{3}$$

For example, Fig. 8 shows the I–V curve of a backward tunnel diode and its current responsivity [61]. For any kind of diode, the polynomial fitting can be used to obtain a function after diode's I-V measurements. Then, diode's current responsivity can be calculated using (3), as presented in Fig. 8. The zero bias current responsivity $R_I|_{(V=0)}$ or R_{I0} is a key parameter that can quantify the nonlinearity of a diode used in low-power rectification. R_{I0} of the backward tunnel diode reaches 21.65 A/W, which is higher than the physical limit of any Schottky diode 19.46 A/W at a room temperature of 25 °C. Schottky diode's R_{I0} can be calculated by:

$$R_{I0} = \frac{q}{2nk_BT} \tag{4}$$

in which q, k_B, and T are electron charge, Boltzmann constant, and operating temperature (in Kelvin). Fig. 8 also shows the physical limits of zero-bias current responsivity of Schottky diodes (assuming a perfect diode ideality $n = 1$) at three different operating temperatures −30 °C, 25 °C, and 80 °C. Low-temperature operation enhances R_{I0}, in other words, the nonlinearity of Schottky diodes. For example, Schottky diodes operating at −30 °C have the potential to outperform the backward tunnel diode in [61].

Based on R_I, the junction conversion efficiency η_0 can be expressed as a function of junction resistance for the low-frequency hypothesis [59]:

$$\eta_0 = \frac{P_{in} R_l^2 R_j^2}{R_l + R_s + R_j} \tag{5}$$

where R_l is load resistance. This explicit conversion efficiency expression indicates that larger input power and stronger nonlinearity will lead to higher conversion efficiency. Therefore, researchers have proposed hybrid energy harvesting technology to obtain more input power, thus leading to higher conversion efficiency. So far, several different forms of ambient energy sources have been involved in hybrid rectification, including solar [56], [62], thermal [3], [63], and mechanical energy [64]. A photo of a hybrid solar-electromagnetic energy harvester is shown in Fig. 6(c) [56].

Besides junction conversion efficiency, the overall rectification efficiency also contains matching network efficiency, parasitic efficiency, and loading efficiency. The rectifier input impedance comprises a reactive (capacitive) component due to the active device capacitance and the various capacitances used in the rectifier circuit [65]. Typically the input impedance of a rectifier circuit at a given input power and output load can be expressed as an equivalent shunt R_eC_e circuit [65]. As a result, impedance matching of the rectifier circuit to the antenna over a large bandwidth represents a significant challenge [66]. The theory developed by Bode and later extended by Fano [67] can be used to compute a minimum reflection coefficient Γ magnitude that can be obtained for a given frequency bandwidth B [66]

$$\Gamma \geq e^{-\frac{1}{2BR_eC_e}}. \tag{6}$$

Fig. 10 presents the state-of-the-art rectification efficiency as a function of operating frequency and input power. Higher efficiency can be obtained at higher power and lower operating frequency.

Novel technologies and techniques are under development in an attempt to maximize rectification efficiency. Section V

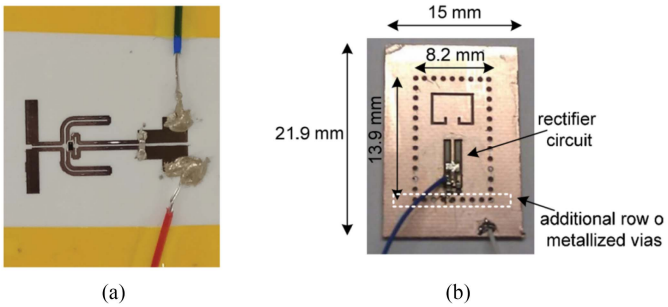

FIGURE 9. (a) 24 GHz rectenna on commercial photo paper substrate and (b) 24 GHz substrate integrated waveguide (SIW) rectenna. After [68], [70].

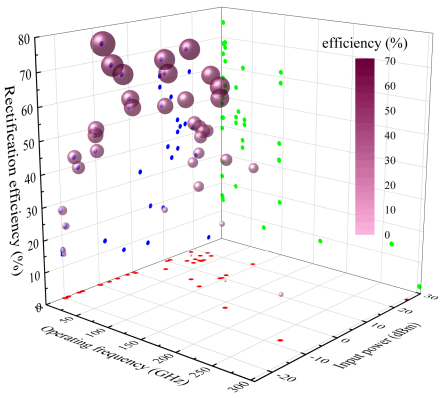

FIGURE 10. State-of-the-art rectification efficiency versus operating frequency and input power [79], [80], [81], [82], [83], [84], [85], [86], [87], [88], [89], [90], [91], [92], [93], [94], [95], [96], [97], [98], [99], [100], [101], [102], [103], [104], [105], [106], [107], [108], [109], [110], [111]. References are listed from lowest to highest operating frequency. Blue, green, and red dots are the projections of efficiency results on three surfaces.

TABLE 2. Rectification Efficiency of Multi-Band Rectifiers for RF EH and WPT Applications

Ref.	Freq. (GHz)	Diode	RF-to-dc conversion efficiency
[55]	0.915/2.45	SMS7630	37% (-9 dBm) @0.915 GHz/ 20% (-15 dBm) @2.45GHz
[56]	0.85/2.45	SMS7630	18% (-20 dBm) @0.85 GHz/ 10% (-20 dBm) @2.45GHz
[115]	0.9/1.8	HSMS2850	13.2% (-30 dBm) @0.9 GHz/ 8% (-30 dBm) @2.45GHz
[116]	0.9/1.8/2.45	HSMS2852	33.7% (-10 dBm) @0.9 GHz/ 22% (-10 dBm) @1.8GHz/ 20% (-10 dBm) @2.45GHz

is dedicated on the design of flexible rectennas, while Fig. 9 shows two rectennas operating 24 GHz, the first one is fabricated on a commercial photo paper substrate and the second one is based on substrate integrated waveguide (SIW) technology [68], [69], [70].

To increase the harvested power level of RF EH systems, multi-band and broadband rectifiers have been investigated in various frequency bands, such as for example in [51], [55], [66], [71], [72], [73]. A selection of rectifiers tailored for WPT and RF EH applications is summarized in Table 2 showing

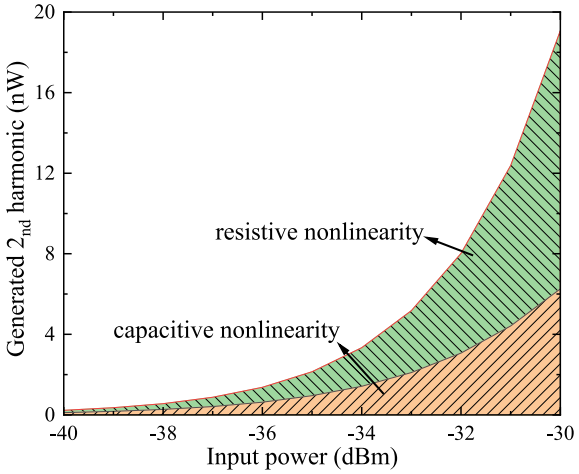

FIGURE 11. Contribution comparison of nonlinear junction resistance and capacitance during second-harmonic generation for a Schottky diode SMS7630 at 3.5 GHz. Note that this is a stacked plot.

the highest rectification efficiency obtained for each design. Furthermore, motivated by the need for high rectification efficiency, high peak-to-average power ratio (PAPR) signals have been tested. It is shown that high PAPR signals lead to higher RF–to-dc conversion efficiency if compared to a CW signal of the same average power [74], [75].

To cope with the low dc voltage generated under low power condition, three techniques are typically implemented. The most common practice is to use a Dickson charge pump [76]. In some more complex energy harvester, a dc-to-dc converter can be used [14], [77]. Finally, some designs also propose to operate RF frontend with hundreds of millivolts, so that the rectifier output voltage could be used without any boost (and efficiency deterioration) [78].

Apart from being the core component in rectifiers, diodes are also commonly used in harmonic backscattering technology, where both nonlinear junction resistance and capacitance contribute to harmonic generation (usually the second-harmonic component). Harmonic backscattering is a fully passive RFID technology that receives RF input and reflects generated second-harmonic signals. For Schottky diodes, analysis can also start from its I-V relationship in (1). Thus, the second-harmonic current due to junction resistance and capacitance can be obtained as [112], [113]:

$$I_{Rj} = \frac{I_s V_{on}^2}{4(nV_t)^2} \tag{7}$$

$$I_{Cj} \approx -\frac{C_{jo} M V_{on}^2 \omega_o}{2V_j} \tag{8}$$

in which M, V_j, and ω_o are diode grading coefficient, junction potetntial, and angular frequency of RF input signal, respectively. To achieve higher conversion efficiency, in other words, to reduce conversion loss, diodes with larger R_{j0} (lower I_s) and smaller C_{j0} are desired. Fig. 11 demonstrates the contribution comparison of junction resistance and capacitance during

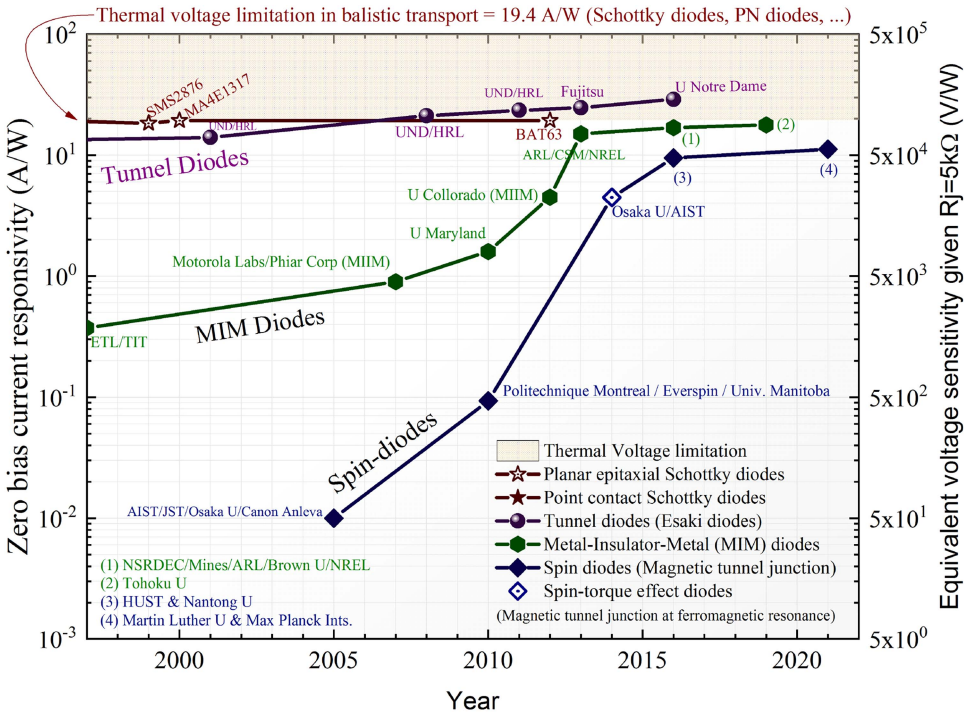

FIGURE 12. **Nonlinearity of diodes over the past 25 years. The most universal parameter to describe the ability to convert energy to harmonics is the current responsivity R_I [A/W]. However, devices are more commonly specified by their voltage sensitivity R_V [V/W], calculated by V_{DC}/P_{in}. At low frequency, $R_V = R_I \cdot R_j$.**

second-harmonic generation for Skyworks SMS7630 diode at 3.5 GHz [112].

The conversion efficiency of ambient energy harvesting is strongly tied to the rectifier nonlinearity at zero bias. This is a parameter to which the research community has been dedicating numerous efforts over the years (see Fig. 12), which can fall into three categories:

A. METAL–SEMICONDUCTOR JUNCTION (SCHOTTKY DIODES)

At a Schottky contact, the electron flow is regulated by the barrier height (which consists of the difference between the interfacial conduction band edge and the Fermi level EF). To pass over the barrier, the electron must be thermally excited, which is done by applying a voltage or by ambient temperature. This latter physical property, unfortunately, is tying the maximum nonlinearity of a device to its operating temperature. In this regard, the only solution to improve the nonlinearity of ballistic transport zero-bias nonlinear devices is to reduce the temperature, as shown in Fig. 8 [11].

B. TUNNELING JUNCTIONS (MIM, TUNNEL DIODES...)

Tunneling transport–induced nonlinear devices present the significant advantage of being insensitive to the operating temperature at zero bias. This enables the technology to outperform Schottky and PN junctions [61]. Current developments include engineering the anode and cathode composition, as well as the junction area [61].

C. MAGNETIC TUNEEL JUNCTION (MRAM, SPIN DIODE)

Spintronics-engineered junctions are probably the most advanced technology that can be harnessed for low-power energy conversion: in addition to the good performance yielded by tunneling transport, the control of the tunneling electron's spin is promising to have a new degree of freedom to achieve greatly nonlinear diodes [114]. Since this is a very new technology (Nobel prize in Physics awarded in 2007), early improvements have grown exponentially, but current research is still working to break the glass ceiling of the Schottky diode's physical limitation. Two research directions here are: (i) the improvement of the overall nonlinearity and (ii) forward-reverse asymmetry.

V. FLEXIBLE RECTENNAS

Significant efforts are currently conducted to develop energy-autonomous low-power wireless transponders on flexible and green materials [4], [117], [118]. Conformable circuits based on flexible substrates can be easily applied to various objects, and even packages, which ease IoT nodes integration with the tagged items. Also, the environmental impact of electronics must be taken into consideration: the life cycle and material characteristics of IoT nodes should match that of the hosting object, to avoid recyclability issues and reduce e-waste. Therefore, flexible rectennas have been investigated.

In the energy harvesting context, since the direction of arrival of the RF power is not known in advance and also the frequencies of the RF signals available in the environment is

(a) (b)

FIGURE 13. Rectenna on paper for Wi-Fi band. (a) Top view, and (b) bottom view. Area: 4.9 × 5.4 cm^2. Weight: 2 grams. After [122].

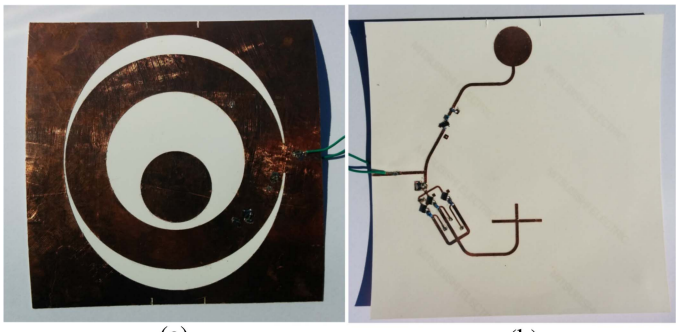

(a) (b)

FIGURE 14. Multi-band rectenna on paper. (a) Top view, and (b) bottom view. Area: 11 × 11 cm^2 Weight: 6 grams. After [124].

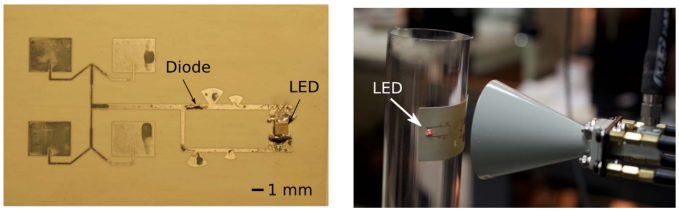

FIGURE 15. Rectenna on liquid crystal polymer substrate at 24 GHz. After [126].

variable, broadband and multi-band rectennas based on low directive radiators are developed [119], [120], [121].

In Fig. 13, a rectenna manufactured on a flexible paper substrate using copper adhesive laminate is illustrated [122]. The rectenna is designed to cover the ISM band from 2.4 to 2.49 GHz. It is based on a tapered annular slot antenna (result of the intersection of an ellipse and a circle) fed by a proximity coupled microstrip line terminated on a circular stub. The rectifier is an envelope detector based on a single series-connected Schottky diode (model HSMS2850) and a distributed input matching network and harmonic termination section. Since the currents excited by the annular slot antenna decay exponentially at the borders of the slot, the metal area surrounding the slot can be used as ground plane for the rest of the microstrip circuit without interfering with the antenna operation. This guarantees high compactness (the rectifier is placed on the interior of the annular slot; therefore, the rectenna area is the same as the antenna area). The rectenna achieves an RF-to-dc conversion efficiency higher than 26 % in all operating band for an incident power density as low as 1.6 μW/cm^2. The corresponding output voltage is about 170 mV, which can be used to power ultra-low voltage electronics [123].

A multi-band version of the previous design has been investigated as well, aimed at covering all LTE bands [124]. This prototype, shown in Fig. 14, consists of two nested annular slot antennas: the outer one is similar to the afore described one and covers the band 790–960 MHz. The inner slot instead is a circular slot with a cross-shaped feed line and a circular patch radiator, offset with respect to the center of the slot. This antenna is broadband and covers the frequency range 1.71–2.69 GHz. Each antenna is connected to its own rectifier: the rectifier connected to the outer slot is a simple envelope detector, while the rectifier connected to the broadband inner slot consists of three branches of envelope detectors connected in parallel, where each branch is optimized to operate in a sub-band of the antenna. To guarantee that each signal is rectified by the branch optimized for its frequency band, one transmission line section is inserted at the input of each branch. This way, the input impedance of the branch is rotated towards high impedance for the frequencies outside its operating band. Both rectifiers are placed on the metal area between the two slots, and are dc-connected in parallel. The rectenna features an RF-to-dc conversion efficiency of 40% at 900 MHz and of about 20% in the higher frequency range for an incident power density of 1 μW/cm^2. This corresponds to an output voltage higher than 180 mV in all bands.

Some studies have been carried to realize flexible rectennas working at mim-waves [125], [126]. Fig. 15 shows a rectenna working at 24 GHz [126]. The rectenna is manufactured on a commercial flexible liquid crystal polymer substrate and the metal traces are ink-jet printed using silver nanoparticle ink. The antenna consists of a 2 × 2 planar patch array. The rectifier consists of a via-less envelope detector based on a ring-shaped circuit topology: using shunt-connected quarter-wave open-circuited radial stubs a virtual short-circuit for the fundamental and the second harmonic components is achieved, while the generated dc component circulates in the ring structure (closed path). To prove the concept, the rectenna was used to switch on an LED under bending conditions.

Rectennas on flexible substrates are also being combined in rectenna arrays to increase the output dc power for large area electronics applications [127], [128]. The six-element rectenna array designed on a polyimide substrate in [128] for example, is used to power a Bluetooth low energy node from an incident power density as low as 0.25 μW/cm^2.

VI. WPT TRANSMITTER

Wireless Power Transmission (WPT) systems can generate higher power density levels compared with RF EH systems.

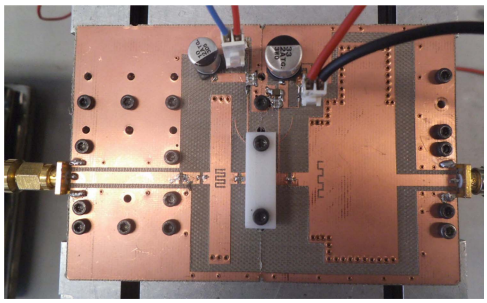

FIGURE 16. Example of a dual-band power amplifier tailored for far-field wireless power applications. After [134].

Information about the regulations and standards on the allowed transmitted levels can be found in [28], [35], [129]. A lot of research has focused on improving the performance of the transmitter in far-field WPT systems.

The end-to-end efficiency of a far-field WPT is defined as the product of each subsystem's efficiency, e.g. transmit efficiency, free-space propagation (channel) efficiency and the power receiver efficiency [2], [9], [130]. The channel efficiency depends on antenna's gain, propagation channel properties, the power transmitter-receiver distance and the operating frequency [51].

The efficiency of a WPT transmitter is a function of the power amplifier (PA) stage performance [130]. Oscillators and PA efficiency dominate WPT transmitters performance. Power amplifier efficiency is a function of the transmitted power level, the selected technology and the operating frequency [2], e.g. [51] presents the analysis of the end-to-end efficiency of a mm-wave WPT system. Fig. 16 shows a photo of a dual-band (2.45 and 5.8 GHz) power amplifier based on substrate integrated waveguide technology tailored for WPT applications.

Fig. 17 presents the block diagram of a high power WPT transmitter along with its receiver for wirelessly charging mobile devices, such as cellphones [37]. One of the main technical challenges for such a system is the low beam efficiency. Quasioptical (QO) theory is adopted in [131] and [132] and to improve the beam efficiency. At the transmitter side, a 4 × 4 5.8 GHz microstrip patch antenna array of 16 active and independent channels with beamforming and beamsteering capabilities with an output power level in the range of 25 W and 32 W is adopted [6], [133]. A 5.1 GHz Local Oscillator (LO) and an Intermediate Frequency (IF) of 0.7 GHz is used; the later is up-converted by a mixer to 5.8 GHz. 16 IQ modulators are used for controlling the amplitude and the phase difference.

A calibration is necessary to account for the gain, attenuation and phase discrepancies. The resulting look-up table is used to adjust the radiation pattern towards the desired direction. At the receiver side, backscattering is used to improve the system's performance. The implemented system highlighting the main components is shown in Fig. 18. Furthermore, the electromagnetic radiation can not be precisely represented by thin rays and has to be compared to Gaussian beams. The fundamentals of gaussian beams can be found in [131].

TABLE 3. Simulation Results of the Standalone Phased-Array (T_x) and the Simulation Results of the Phased-Array and Lens Radiating System (T_x + Lens)

Beam waist location	Gain [dBi]		Efficiency [%]	
	T_x	T_x + Lens	T_x	T_x + Lens
Infinity	18.42	24.25	84.17	84.62
1000 mm	18.34	23.92	84.16	84.51
500 mm	18.02	23.36	84.08	84.09
400 mm	17.77	22.99	84.01	83.78
300 mm	17.23	22.25	83.87	83.12
200 mm	15.72	20.35	83.45	81.52

The coupling efficiency [135], [136] is an important antenna metric and can be calculated as below:

$$\eta_G = \frac{\iint \left|E_A \cdot E_G^*\right|^2 dx\, dy}{\left[\iint |E_A|^2 dx\, dy\right]\left[\iint |E_G|^2 dx\, dy\right]} \tag{9}$$

Fig. 19 presents the results from a full scanning range analysis evaluating the performance and the beamforming capabilities of the array. Fig. 19(a) and (b) show that the transmitter can radiate in several azimuth and elevation angles from −60° to +60°, respectively. The received power for different phase configurations of the active phased array, while the mobile device and feedback channel are physically moved in the anechoic chamber, are shown in [37].

To maximize the beam efficiency, the energy must be focused through dielectric lens. Spherical and elliptical surface lens are used to reduce its reflectivity [131], [137]. The presented design is based on the principles found in [137], where the lens' diameter and thickness is related to its focal length. The obtained results are summarized in Table 3.

Despite the beam directivity offered from the dielectric lens usage, a further analysis of the gaussian beam is required to determine the beam from the phased array. A key challenge here is the limited beamsteering (e.g. the beam might miss the lens at some distance from the phased array at extreme angles). While using a lens improves the beam efficiency, the trade-off between beam steering and beam focusing requires further investigation.

VII. MM-WAVE WIRELESS POWER TRANSFER

A. MM-WAVE POWER

As enticing as the prospect of wireless power transfer, either intentional in WPT systems or opportunistic in EH systems, the broad commercial deployment of products enabled with such capabilities has been hampered by performance limitations. Indeed, on the one hand are the physical limitations of diode-based rectifiers [138] and of the unavoidable power dilution effect suffered in the wireless antenna-to-antenna links while, on the other hand, are the regulatory impediments placed by organizations like the Federal Communications Commission, FCC, in the USA, which limit both

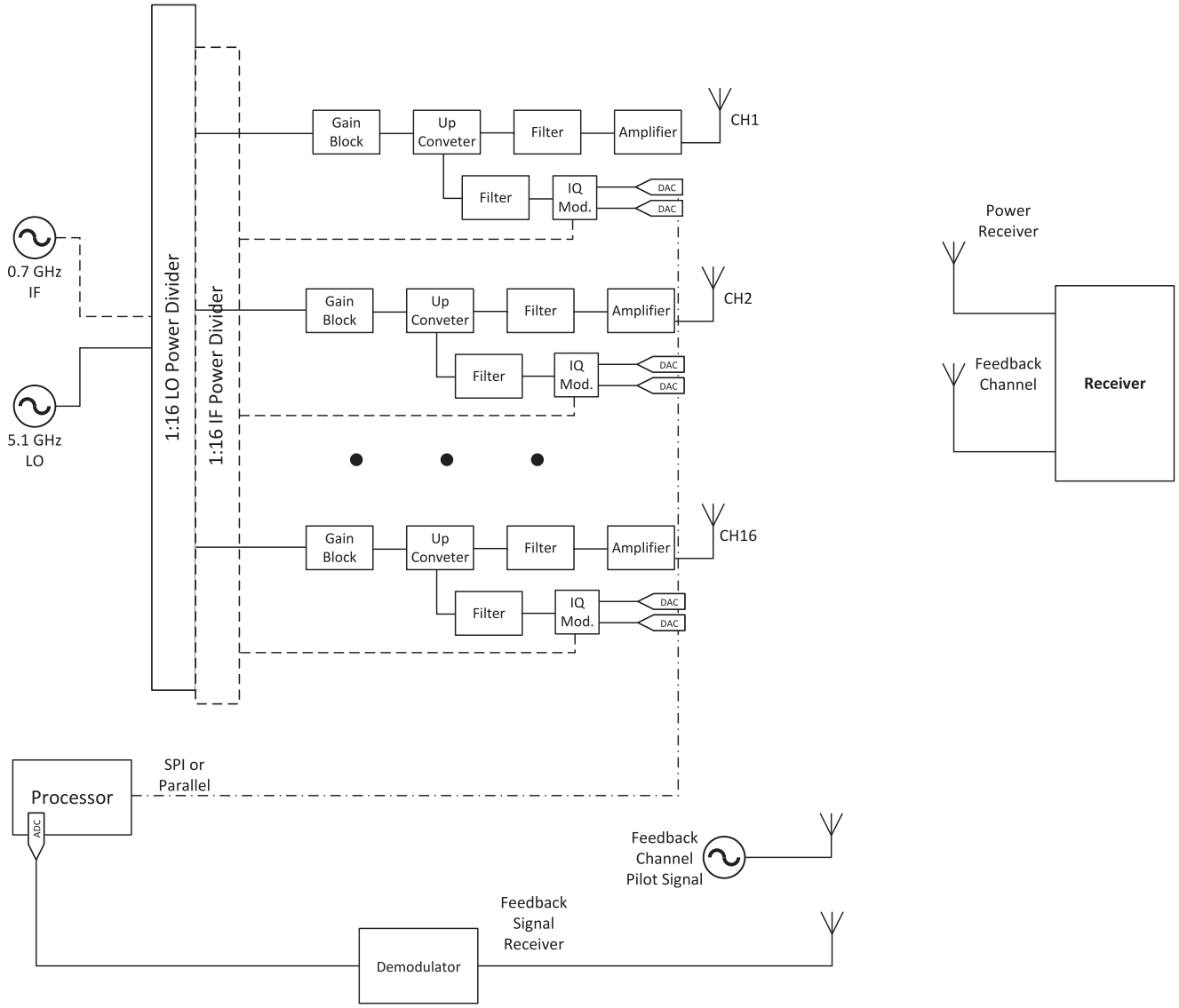

FIGURE 17. Block diagram of the Wireless Power Transfer (WPT) system setup as presented in [37].

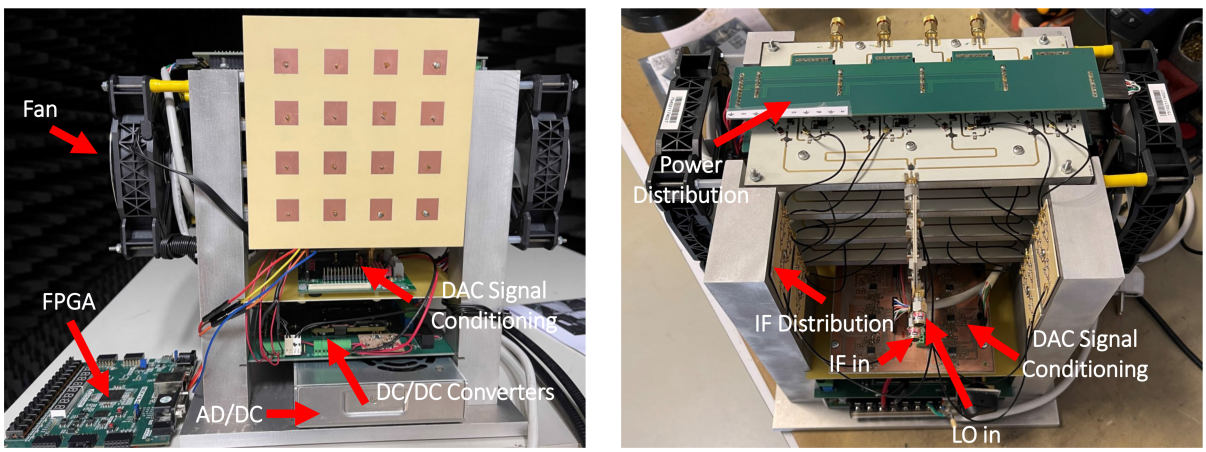

FIGURE 18. Photograph of the transmitter and its sub-components front and back of the transmitter setup as presented in [37].

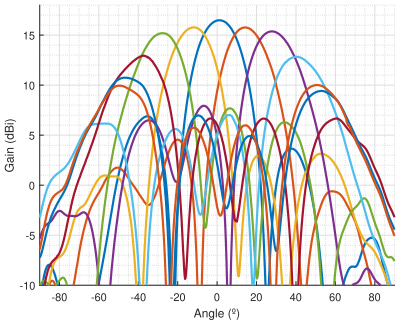

(a)

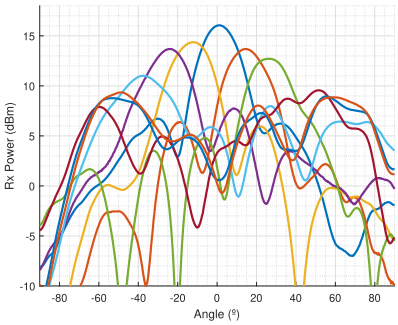

(b)

FIGURE 19. **(a) Radiation pattern (full scan) in the azimuth plane and (b) radiation pattern (full scan) in the elevation plane of the work presented in [37].**

the amount of radiated power and the power densities (through Effective Isotropic Radiated Power (EIRP) limits) that one is able to transmit. For example, an unlicensed system operating in the ultrahigh frequency range (UHF) band and allowed up to 36 dBm in EIRP needs to deliver about at least −30 dBm at the input of a remote rectifier to generate any sort of usable output dc power. In order to put these numbers into perspective, one should take into account that the most common commercial types of wirelessly-powered systems (UHF RFIDs) require powers in excess of −25 dBm to turn on, although state-of-the-art rectifiers with efficiencies of −30.7dBm at 2.4 GHz have been reported [139].

Using Friis' transmission equation [140]

$$P_r = P_e \frac{A_r G_t}{4\pi R^2} = \text{EIRP} \frac{A_r}{4\pi R^2} \tag{10}$$

where R, P_e, P_r, A_r, and G_t are, respectively, the range between the transmitted and the receiver, the emitted power, the received power, the physical aperture of the reader antennas, and the gain of the tag antenna respectively, one can calculate the maximum range achieved by an ideal system transmitting an EIRP of 36 dBm such that −30 dBm are received by perfectly-efficient antenna of a reasonable 5 cm by 5 cm size: the answer is 28 m. This value represents an upper bound. Once the imperfections of real antennas are accounted for, such as the antenna efficiency and polarization mismatch between the transmit and receive antennas, this value is quickly reduced below 20 m. These estimates are consistent with the known performance of commercial UHF RFIDs [140].

A better alternative lies in the utilization of licensed cellular bands. Traditional cellular base-stations are rather ubiquitous and are allowed to emit 55 dBm EIRP. With such capabilities, a similar theoretical exercise reveals potential powering ranges of approximately 250 m. However, cellular cell sizes typically exceed 1 km in radius, thereby leaving gaping holes in potential power coverage, let alone the influence of multipath and obstacles.

Is this the end of the story? It could have been without a nascent disruptive force in cellular networks: 5G. 5G, in its FR2 mm-wave form, has been granted for its base-stations the ability to emit up to 75 dBm of EIRP. With such a power, a system such as the one analyzed in the previous paragraphs could be powered at a distance of 1.7 km, a range far exceeding the standard cell size of 200 m envisioned for such systems. This realization, first reported in [141], does not come without its challenges. Indeed, at the frequencies exceeding 28 GHz used by 5G, the realization of large (of the 5 cm by 5 cm aforementioned dimensions), efficient, and direction-agnostic antenna systems provided that such high EIRP values require an extremely precise alignment between the transmit and receive antennas, along with that of rectifiers capable of operating down to the −30 dBm sensitivities of their lower-frequency counterparts is non-trivial and may, even, seem impossible. It is to the early attempts at solving these technical challenges that the following section is dedicated.

B. POWERING NEXT GENERATION RFID SYSTEMS WITH 5G MM-WAVE POWER

The large EIRPs allowable by the FCC in the licensed 5G bands have stimulated innovations in the design of mm-wave-enabled powering and backscattering communications solutions. While some works focused on improving the rectification efficiency or sensitivity via the design of Schottky diode-based rectifiers [70], [95], [142] or Complementary Metal–Oxide–Semiconductor (CMOS) systems [143], [144], others focused on solving a fundamental problem that occurs at mm-waves: the inability to achieve high gains with large antenna array structures while maintaining a wide angular coverage [141]. To better explain the need for such capabilities, we show in Fig. 20 how a 5G base station would steer its beam in multiple directions to energize IoT devices.

If the device is equipped with a conventional array structure, its high gain pencil-beam radiation pattern would not be capable to receive the signals coming from oblique angles, rendering their deployment extremely impractical in any environment. If, however, the IoT devices are equipped with structures that could enable a wide field of view while maintaining the large gain, necessary for long ranges, devices can then be energized by waves impinging from any direction as shown in Fig. 20.

Motivated by this need, the authors in [141] proposed a system that could bring the 5G wireless power grid concept to

FIGURE 20. Schematic showing a 5G/mm-wave base station steering its beam to energize and communicate with IoT devices.

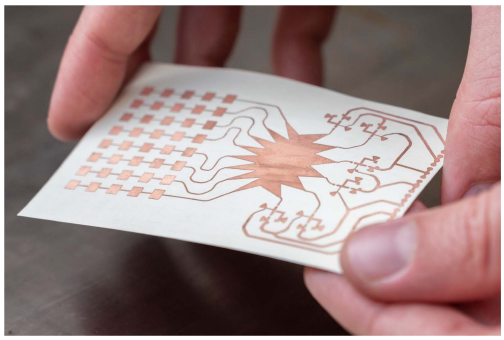

FIGURE 21. Photo of the planar Rotman lens-based RF energy harvester.

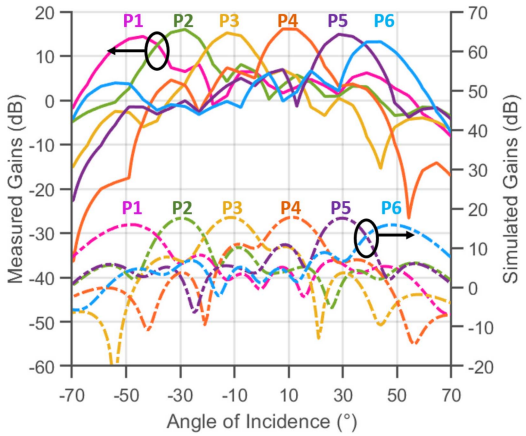

FIGURE 22. Measured and simulated gain values at all six ports (P1 to P6) of the Rotman lens-based antenna array proposed in [146].

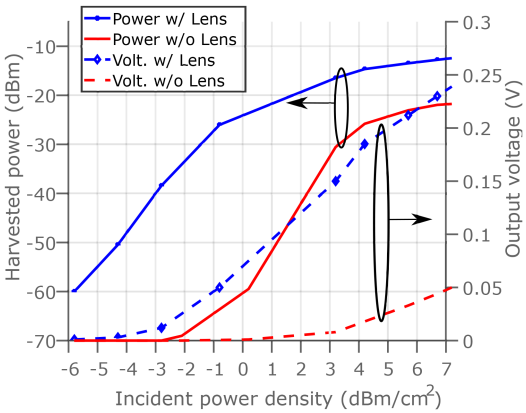

FIGURE 23. Plot of the measured voltages and output powers versus incident power density for the rectenna with and without the Rotman Lens as presented in [147].

reality. Far from conventional array designs, the research took advantage of a passive beamforming network (BFN) structure, the Rotman lens, first introduced in the 1960's [145]. This microwave lens-based network constitutes one of the most cost-effective designs for BFNs, capable of passively enabling multibeam phased array system over a wide band of frequencies, thanks to its implementation of true-time-delays. The Rotman lens is surrounded by two angles of curvature, accounting for the antenna ports on one side and the beam ports on the opposite side. Designers can change the number of ports on both ends to control the gain, angular coverage and overall performance of the lens. Based on a scalability study the authors conducted in [141], a Rotman lens with eight antenna ports and six beam ports was found ideal to achieve a good gain and wide angular coverage.

Fig. 21 shows the photo of the fabricated Rotman lens-based mm-wave harvester. The structure is composed of eight serially-fed linear patch antenna arrays connected to the Rotman lens on one end, while six 28 GHz rectifiers were placed at the beam ports. With a wave impinging from any direction, all the antennas scavenge the signals and feed them to the Rotman lens that combines them internally and focuses them to a single beam port, also called focal point. By placing a rectifier on each one of these ports, the structure ensures the arrival of maximum power at the input of that rectifier. The simulated and measured gains on all six ports of the Rotman lens are shown in Fig. 22, demonstrating the Rotman-based array capabilities in achieving a high gain of 17 dB and a simultaneous wide angular coverage of 120 °.

The superiority of the Rotman lens-based rectenna was also demonstrated over a conventional rectenna that does not include the lens. Both structures were designed on the same substrates (180 μm thin and flexible Liquid Crystal Polymer: LCP), fabricated using an inkjet printer, and tested with respect to incident power densities and angles of incidence [147]. The plot shown in Fig. 23, displays the measured harvested powers and output voltages of the two structures with and without the lens. Since the Rotman lens combines the power coming from all antennas to one port, it can be seen how it enables a higher rectenna turn-on sensitivity and rectification efficiency compared to the lensless rectenna.

It should be noted that the concept of lens based rectenna arrays is not new as it has been applied in imaging systems, however its application in energy harvesting and wireless power transfer applications has been considered to the best of our knowledge in 5G millimeter wave systems in [141]. Another beam forming based rectenna array has been proposed in [148], where a Butler matrix based rectenna array

at 2.4 GHz has been demonstrated. Furthermore, in [149] the concept of staggered arrays has been proposed, where sub-arrays of rectennnas are configured to point to different directions in the horizon.

The work of [150] demonstrated that it is possible to enable long range mm-wave harvesting promising the delivery of multiple μWs of power at ranges exceeding 180 m, the 5G cell size, using the full 75 dBm EIRP allowable by the FCC in the 5G/mm-wave bands. Advances in mm-wave backscattering solutions, a.k.a mmIDs [151], manifested through the ultra-long km-range communications, ultra-low-power (μW level), and retrodirective capabilities (Van Atta and Rotman lens-based mmIDs) [146], [152], [153], coupled with the 5G powering solution described here, enable the emergence of fully-passive mmIDs for digital twinning applications in smart cities and infrastructures.

VIII. SIMULTANEOUS WIRELESS INFORMATION AND POWER TRANSFER (SWIPT)

In this last decade, techniques for simultaneous wireless information and power transfer (SWIPT) have attracted an increased interest for a wide range of applications such as RFIDs [34]. This section summarizes some near-field and far-field recent developments on SWIPT.

An interesting demonstration of a moving WPT system for industrial applications is described in [154]. The system operates at 6.78 MHz and consists of a modular architecture of small resonant series-connected TX coils (Fig. 24(a)), designed together with the receiver in such a way that it is able to guarantee constant dc voltage at the output of a sliding RX, independent from the misalignment (see output voltage in Fig. 24(b)).

A set of gallium nitride (GaN)-based coupled load-independent Class EF inverters are designed for the same output current in such a way that each coil is "virtually" series-connected to the closely located ones, that is the most robust set up with respect to misalignements. The RX coil is connected to a passive Class E rectifier, which is designed to maintain a constant dc output voltage regardless of load or position. Comprehensive empirical results are shown to demonstrate performance under various loading conditions and positions. For a dc output power of 100 W, a peak dc-to-dc efficiency of 80% is achieved, and a dc output voltage variation less than 5% is measured, over a load range of 30 to 500 Ω. The base operating principles have been exploited in [155] where the series-connected TX coils, is designed to resonate at 100 kHz, allowing data transfer while maintaining a high-efficient wireless power transfer thanks to the strong coupling between the TX coils and the receiving one, over the entire track.

By embedding in the same structure a ultrahigh frequency range (UHF) communication system, an original implementation of NF-SWIPT in automatic machinery has been demonstrated in [156]. For data communication, the system uses a self-resonant near-field link based on the coupling of two split ring resonators (SRRs), co-located with the inductive power

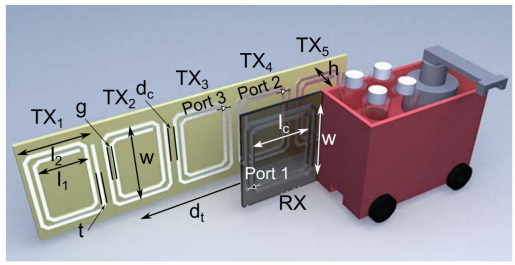

(a)

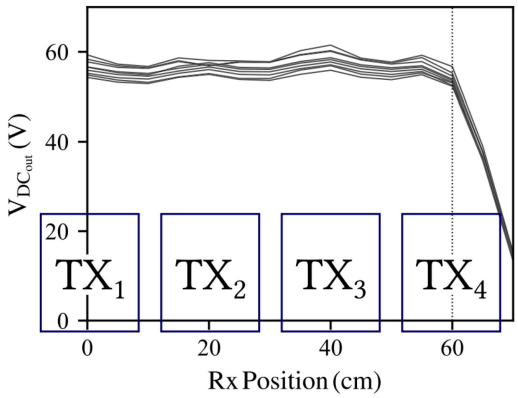

(b)

FIGURE 24. (a) Pictorial representation of the link setup and (b) measured dc-output voltage with respect to different positions of the receiving coil, as presented in [154] © IEEE 2017.

transfer link operating at 50 kHz, as illustrated in Fig. 25(a). The two SRRs are separated by a distance d of few millimeters whereas α describes the rotation. Fig. 25(b) provides a schematic representation of the SWIPT device with details on the stack-up.

Among several applications of SWIPT paradigms, localization can be annumerated, especially when operating in far-field. In [157], a chipless solution exploits multisine excitation at UHF, typically adopted for improving the rectifier RF-to-dc efficiency, for generating a passive UWB pulse while performing energy harvesting. The circuit implemented in [157] is shown in Fig. 26(a).

The simulated approach has been shown to be innovative from the computational time point of view: in particular, the portrayal of the multisine as a periodic excitation rather than a quasi-periodic one, with each tone corresponding to a higher harmonic of the same fundamental frequency, the tones' spacing f_0, has enabled the capability of achieving an optimized pattern of the multisine signal [157]. Indeed, the proposed procedure allows to efficiently design the multi-tone signal using as optimization variables the number of tones and the frequency spacing, without limitations due to the cumbersome calculations involved in quasi-periodic HB simulations. The computational times for a periodic and a quasi-periodic representation of the UHF excitation are compared in Fig. 26(b) showing the benefit of the proposed approach.

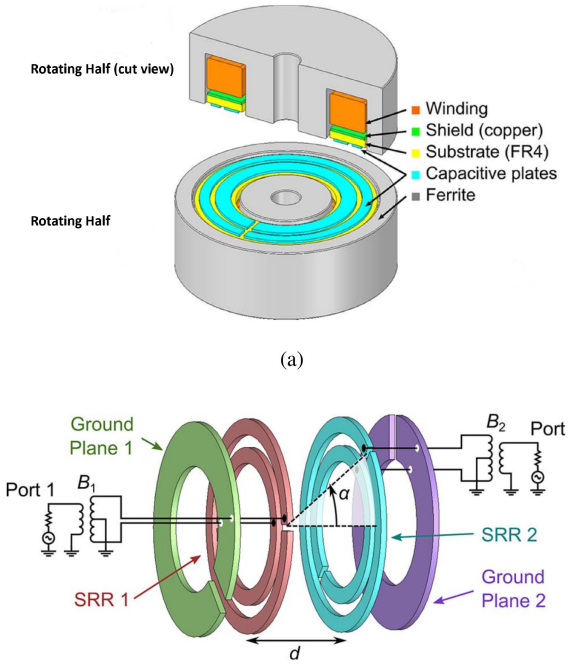

FIGURE 25. (a) Pictorial representation of the SWIPT system with detailed arrangement of the stack-up and (b) schematic representation of the SRR link proposed in [156] © IEEE 2016.

Furthermore, it is demonstrated that increasing the tones spacing allows to further improve localization accuracy: if the multisine excitation bandwidth is 500 kHz, for an observation time $T_{obs} = 500$ ms the reading distance can reach 12 m, whereas when the tone spacing is increased up to 2 MHz, a localization accuracy up to the centimeter-level can be achieved up to 16 m. Fig. 26(c) shows the root-mean-square error (RMSE) for increasing distance between the tag and the receiver for a -10 dBm received power, 8 tones for a $f_0 =$ 500 kHz and $f_0 = 2$ MHz respectively.

In [158], an example of flexible rectenna realized on felt and conductive fabric is presented. Contrary to the previous case, this approach uses far-field for both data and energy transfer by means of a dual-band antenna operating at 2.4 GHz for the off-body communication and a sub-1 GHz (785–875 MHz) rectenna for RF harvesting (Fig. 27). This architecture presents an improvement of 25% of the maximum power conversion efficiency with respect to state-of-the-art sub-μW/cm^2 textile rectennas. This work demonstrates also that SWIPT does not deteriorate the energy harvesting or communications performance.

Antenna design is definitely crucial while dealing with systems that adopt the same frequency band for transferring at the same time data and energy: [159] proposes a two-port (one for EH, one for communication) multi-polarization rectenna, fed by an orthogonal hybrid coupler (Fig. 28).

Based on the coupler symmetry, this architecture allows to achieve multi-polarization modes, and in particular circular polarization (both right-handed and left-handed) for the single-port operation and linear polarization for the two-port operation. This is clearly an advantage for feeding the antenna part of an RFID sensor situated in an electromagnetically uncertain environment as the real world is.

Another interesting way to face this issue, and in particular the antenna polarization uncertainties, has been presented in [160], with the exploitation of the 2^{nd} and 3^{rd} harmonics

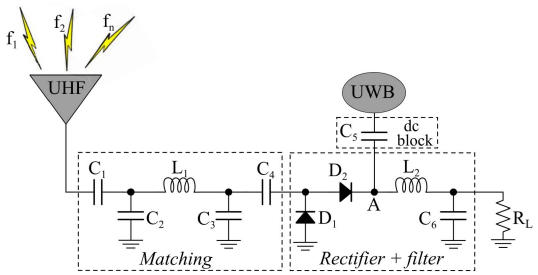

Regime	No. tones	IMD order	No. spectral lines	CPU time (s)
Quasi-periodic	4	6	644	36
Quasi-periodic	8	4	19,912	74,280
Periodic	4	–	6,000	35
Periodic	8	–	6,000	42
Periodic	16	–	6,000	55

(b)

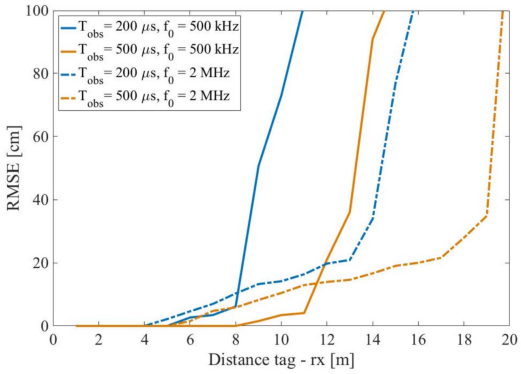

FIGURE 26. (a) Schematic representation of the passive, UWB-pulse generator tag proposed in [157], (b) comparison of computational time for periodic and quasi-periodic analysis and (c) localization RMSE for increasing TX-RX distance [157] © IEEE 2018.

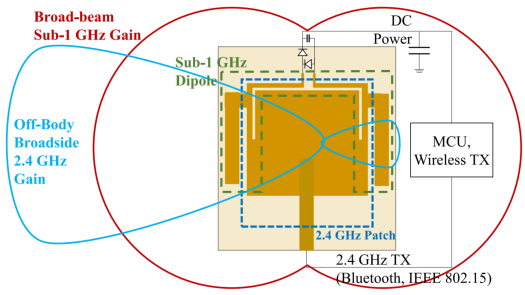

FIGURE 27. Dual-band antenna system for a wearable flexible prototype as presented in [158] © IEEE 2021.

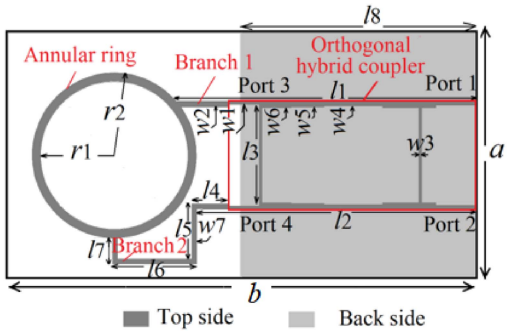

FIGURE 28. Two-port multi-polarization antenna for SWIPT proposed in [159]: overall dimensions: a = 55 mm, b = 105 mm © IEEE 2021.

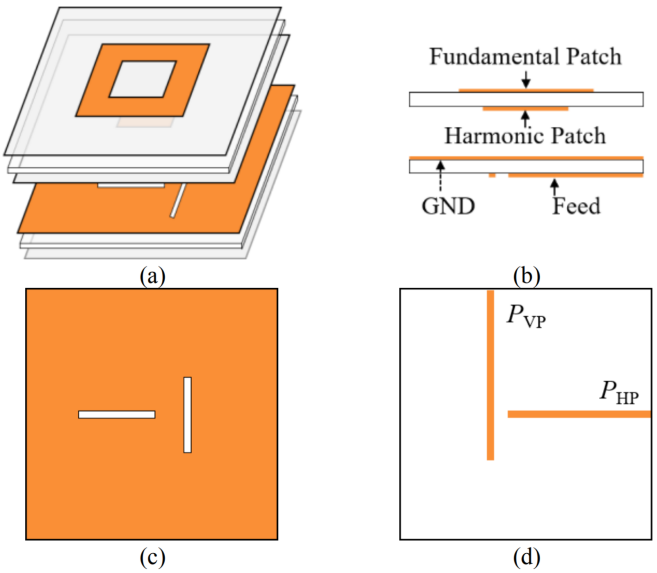

FIGURE 29. Layout of the DLP antenna presented in [160]: (a) exploded view, (b) stack-up, (c) ground layer and (d) feeding layer © IEEE 2021.

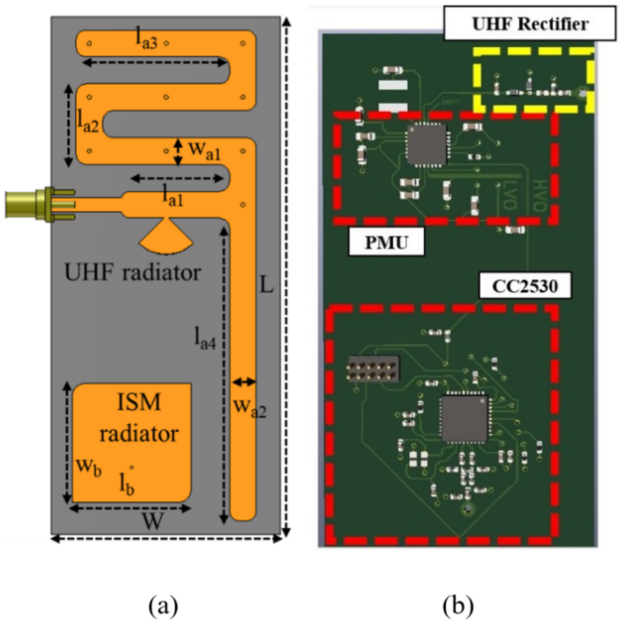

FIGURE 30. (a) Two-port antenna design and (b) overall design of the board for a dual-band RFID SWIPT node proposed in [161] © IEEE 2022.

generated at the output of the RF-to-dc rectifier, which have a monotonic relation with the incident power. In this manner, the harmonics backscattered from the rectenna are used to track variations of the incident power related to antenna polarization and its unknown distance. In this work, a shared-aperture dual-band dual linearly polarized (DLP) antenna is designed (Fig. 29): the slots in the ground plane allow to excite both harmonic and fundamental patches through an air substrate for dual-band radiations.

In [161], a novel architecture for a RFID SWIPT tag is presented, adopting a dual-frequency multiple-input-multiple-output (MIMO) antenna; the 915 MHz radiating element consists of a meandered monopole used for EH, whereas the 2.4 GHz antenna element is a square patch with truncated corners to guarantee the circular polarization (Fig. 30(a)), which is used for data communication. The overall size of the dual-port MIMO antenna (and consequently of the tag itself) is 47 $\times$ 100 mm^2 (Fig. 30(b)). With a storage capacitor of 150 μF, a stored energy of 0.47 mJ is warranted, making possible a single communication cycle of transmission/reception (TX/RX) lasting for a maximum of 3.5 ms.

The exploitation of novel modulation techniques is crucial for a successful exploitation of SWIPT; in that sense, in [162] a novel magnitude ratio modulation is proposed, using a two-tone signal and using the ratio between the two tones as the coding symbols. This work demonstrates the possibility to deliver a constant dc power to the sensors, which has not been demonstrated using other modulation schemes. In fact, if the channel is narrowband, the proposed modulation is not affected by the wireless channel, and a demodulation is possible even without knowing the channel's attenuation. With a received power of -10 dBm the power conversion efficiency is comprised between 46 % and 52 % by changing the symbols. The main drawback of this solution is given by the fact that the receiving sensor, essentially composed of a rectenna, is highly nonlinear and needs a complete characterization in order to correctly demodulate the signal.

IX. CONCLUSION

Several key challenges arise from the exponential growth of low-power wireless devices. RF energy harvesting and wireless power transfer technologies are promising solutions for enabling the future energy autonomous devices. Despite the significant progress made over the past decades, there are still important challenges to overcome and therefore, extensive research is currently performed. This article reviews state-of-the-art technologies and highlights future development opportunities.

In particular, the challenge of high rectification efficiency is discussed, with an emphasis on diode modeling and the available diode technologies. The need for RF surveys to cover

the new 5G frequency bands is highlighted along with the efforts for the design of flexible and environmentally friendly rectennas. Motivated from the ongoing 5G rollout and the presence of RF energy at higher frequency bands, the prospect of utilizing 5G mm-wave power to drive future RFID systems is also discussed. Furthermore, the article reviews promising near-field and far-field simultaneous wireless information and power transfer solutions.

REFERENCES

[1] "IOT ANALYTICS, state of the IoT 2020, Nov. 2020." Accessed Oct. 03, 2022. [Online]. Available: https://iot-analytics.com/state-of-the-iot-2020-12-billion-iot-connections-surpassing-non-iot-for-the-first-time/

[2] A. Georgiadis, A. Collado, and M. M. Tentzeris, *Energy Harvesting: Technologies, Systems, and Challenges* (EuMA High Frequency Technologies Series). Cambridge, U.K.: Cambridge Univ. Press, 2021.

[3] L. Guo, X. Gu, P. Chu, S. Hemour, and K. Wu, "Collaboratively harvesting ambient radiofrequency and thermal energy," *IEEE Trans. Ind. Electron.*, vol. 67, no. 5, pp. 3736–3746, May 2020.

[4] X. Gu, P. Burasa, S. Hemour, and K. Wu, "Recycling ambient RF energy: Far-field wireless power transfer and harmonic backscattering," *IEEE Microw. Mag.*, vol. 22, no. 9, pp. 60–78, Sep. 2021.

[5] J. Garnica, R. A. Chinga, and J. Lin, "Wireless power transmission: From far field to near field," *Proc. IEEE*, vol. 101, no. 6, pp. 1321–1331, Jun. 2013.

[6] C. A. Balanis, *Antenna Theory: Analysis and Design*. Hoboken, NJ, USA: Wiley, 2005.

[7] Z. Popovic, "Near- and far-field wireless power transfer," in *Proc. 13th Int. Conf. Adv. Technol., Syst. Serv. Telecommun.*, 2017, pp. 3–6.

[8] N. B. Carvalho et al., "Wireless power transmission: R&D activities within Europe," *IEEE Trans. Microw. Theory Techn.*, vol. 62, no. 4, pp. 1031–1045, Apr. 2014.

[9] C. A. I. Team, "Europe and the future for WPT: European contributions to wireless power transfer technology," *IEEE Microw. Mag.*, vol. 18, no. 4, pp. 56–87, Jun. 2017.

[10] H. J. Visser, A. C. F. Reniers, and J. A. C. Theeuwes, "Ambient RF energy scavenging: GSM and WLAN power density measurements," in *Proc. 38th Eur. Microw. Conf.*, 2008, pp. 721–724.

[11] X. Gu, D. Dousset, K. Wu, L. Grauwin, and S. Hemour, "Ambient radiofrequency energy mapping of montreal for far-field wireless power harvesting," in *Proc. IEEE Int. Symp. Antennas Propag. North Amer. Radio Sci. Meeting*, 2020, pp. 1577–1578.

[12] R. J. Vyas, B. B. Cook, Y. Kawahara, and M. M. Tentzeris, "E-WEHP: A batteryless embedded sensor-platform wirelessly powered from ambient digital-TV signals," *IEEE Trans. Microw. Theory Techn.*, vol. 61, no. 6, pp. 2491–2505, Jun. 2013.

[13] A. Alex-Amor et al., "RF energy harvesting system based on an archimedean spiral antenna for low-power sensor applications," *Sensors*, vol. 19, no. 6, 2019, Art. no. 1318. [Online]. Available: https://www.mdpi.com/1424-8220/19/6/1318

[14] M. Pinuela, P. D. Mitcheson, and S. Lucyszyn, "Ambient RF energy harvesting in urban and semi-urban environments," *IEEE Trans. Microw. Theory Techn.*, vol. 61, no. 7, pp. 2715–2726, Jul. 2013.

[15] M. A. Andersson, A. Özçelikkale, M. Johansson, U. EngstrÖm, A. Vorobiev, and J. Stake, "Feasibility of ambient RF energy harvesting for self-sustainable M2M communications using transparent and flexible graphene antennas," *IEEE Access*, vol. 4, pp. 5850–5857, 2016.

[16] X. Zhang, J. Grajal, M. López-Vallejo, E. McVay, and T. Palacios, "Opportunities and challenges of ambient radio-frequency energy harvesting," *Joule*, vol. 4, no. 6, pp. 1148–1152, 2020. [Online]. Available: https://www.sciencedirect.com/science/article/pii/S2542435120301896

[17] M. K. Mishu et al., "Prospective efficient ambient energy harvesting sources for IoT-equipped sensor applications," *Electronics*, vol. 9, no. 9, 2020, Art. no. 1345. [Online]. Available: https://www.mdpi.com/2079-9292/9/9/1345

[18] H. Tataria, M. Shafi, A. F. Molisch, M. Dohler, H. SjÖland, and F. Tufvesson, "6G wireless systems: Vision, requirements, challenges, insights, and opportunities," *Proc. IEEE*, vol. 109, no. 7, pp. 1166–1199, Jul. 2021.

[19] B. Clerckx, "The freedom of wireless energy transmission, imperial college." Accessed: Oct. 3, 2022. [Online]. Available: https://www.youtube.com/watch?v=tkj9jszsfg8

[20] C. T. Rodenbeck et al., "Microwave and millimeter wave power beaming," *IEEE J. Microwaves*, vol. 1, no. 1, pp. 229–259, Jan. 2021.

[21] B. Clerckx, A. Costanzo, A. Georgiadis, and N. B. Carvalho, "Toward 1G mobile power networks: RF, signal, and system designs to make smart objects autonomous," *IEEE Microw. Mag.*, vol. 19, no. 6, pp. 69–82, Sep.–Oct. 2018.

[22] B. Clerckx, J. Kim, K. W. Choi, and D. I. Kim, "Foundations of wireless information and power transfer: Theory, prototypes, and experiments," *Proc. IEEE*, vol. 110, no. 1, pp. 8–30, Jan. 2022.

[23] W. Brown, "The history of power transmission by radio waves," *IEEE Trans. Microw. Theory Techn.*, vol. 32, no. 9, pp. 1230–1242, Sep. 1984.

[24] J. Landt, "The history of RFID," *IEEE Potentials*, vol. 24, no. 4, pp. 8–11, Oct.–Nov. 2005.

[25] N. Shinohara, "Power without wires," *IEEE Microw. Mag.*, vol. 12, no. 7, pp. S64–S73, Dec. 2011.

[26] A. Hagerty, D. Joseph, N. D. Lopez, B. Popovic, and Z. Popovic, "Broadband rectenna arrays for randomly polarized incident waves," in *Proc. 30th Eur. Microw. Conf.*, 2000, pp. 1–4.

[27] V. Liu et al., "Ambient backscatter: Wireless communication out of thin air," *ACM SIGCOMM Comput. Commun. Rev.*, vol. 43, no. 4, pp. 39–50, 2013.

[28] N. Shinohara, "History and innovation of wireless power transfer via microwaves," *IEEE J. Microwaves*, vol. 1, no. 1, pp. 218–228, Jan. 2021.

[29] H. J. Visser, "A brief history of radiative wireless power transfer," in *Proc. 11th Eur. Conf. Antennas Propag.*, 2017, pp. 327–330.

[30] T. S. C. Rao and K. Geetha, "Categories, standards and recent trends in wireless power transfer: A survey," *Indian J. Sci. Technol.*, vol. 19, no. 20, pp. 1–11, 2016.

[31] "Wireless power transfer history and state-of-the-art." Accessed: Oct. 3, 2022. [Online]. Available: https://wpt.ieee.org/wpt-history

[32] N. Shinohara and J. Zhou, *Far Field Wireless Power Transfer and Energy Harvesting*. Norwood, MA, USA: Artech House, 2022.

[33] W. Brown and E. Eves, "Beamed microwave power transmission and its application to space," *IEEE Trans. Microw. Theory Techn.*, vol. 40, no. 6, pp. 1239–1250, Jun. 1992.

[34] A. Costanzo, D. Masotti, G. Paolini, and D. Schreurs, "Evolution of SWIPT for the IoT world: Near- and far-field solutions for simultaneous wireless information and power transfer," *IEEE Microw. Mag.*, vol. 22, no. 12, pp. 48–59, Dec. 2021.

[35] J. Huang, Y. Zhou, Z. Ning, and H. Gharavi, "Wireless power transfer and energy harvesting: Current status and future prospects," *IEEE Wireless Commun.*, vol. 26, no. 4, pp. 163–169, Aug. 2019.

[36] N. Shinohara, "Trends in wireless power transfer: WPT technology for energy harvesting, mllimeter-wave/THz rectennas, MIMO-WPT, and advances in near-field WPT applications," *IEEE Microw. Mag.*, vol. 22, no. 1, pp. 46–59, Jan. 2021.

[37] D. Matos et al., "Charging mobile devices in indoor environments," *Energies*, vol. 15, no. 9, 2022, Art. no. 3450. [Online]. Available: https://www.mdpi.com/1996-1073/15/9/3450

[38] W. Hong et al., "The role of millimeter-wave technologies in 5G/6G wireless communications," *IEEE J. Microwaves*, vol. 1, no. 1, pp. 101–122, Jan. 2021.

[39] S. Kitazawa, H. Ban, and K. Kobayashi, "Energy harvesting from ambient rf sources," in *Proc. IEEE MTT-S Int. Microw. Workshop Ser. Innov. Wireless Power Transmiss.: Technol., Syst., Appl.*, 2012, pp. 39–42.

[40] U. Muncuk, K. Alemdar, J. D. Sarode, and K. R. Chowdhury, "Multiband ambient RF energy harvesting circuit design for enabling batteryless sensors and IoT," *IEEE Internet Things J.*, vol. 5, no. 4, pp. 2700–2714, Aug. 2018.

[41] X. Gu, L. Grauwin, D. Dousset, S. Hemour, and K. Wu, "Dynamic ambient RF energy density measurements of montreal for battery-free IoT sensor network planning," *IEEE Internet Things J.*, vol. 8, no. 17, pp. 13209–13221, Sep. 2021.

[42] D. Belo, A. Georgiadis, and N. B. Carvalho, "Increasing wireless powered systems efficiency by combining WPT and electromagnetic energy harvesting," in *Proc. IEEE Wireless Power Transfer Conf.*, 2016, pp. 1–3.

[43] I. D. Bougas, M. S. Papadopoulou, K. Psannis, P. Sarigiannidis, and S. K. Goudos, "State-of-the-art technologies in RF energy harvesting circuits–a review," in *Proc. 3rd World Symp. Commun. Eng.*, 2020, pp. 18–22.
[44] M. Cansiz, D. Altinel, and G. K. Kurt, "Efficiency in RF energy harvesting systems: A comprehensive review," *Energy*, vol. 174, pp. 292–309, 2019.
[45] B. Clerckx, R. Zhang, R. Schober, D. W. K. Ng, D. I. Kim, and H. V. Poor, "Fundamentals of wireless information and power transfer: From RF energy harvester models to signal and system designs," *IEEE J. Sel. Areas Commun.*, vol. 37, no. 1, pp. 4–33, Jan. 2019.
[46] A. Costanzo et al., "Electromagnetic energy harvesting and wireless power transmission: A unified approach," *Proc. IEEE*, vol. 102, no. 11, pp. 1692–1711, Nov. 2014.
[47] M. Wagih, A. S. Weddell, and S. Beeby, "Rectennas for radio-frequency energy harvesting and wireless power transfer: A review of antenna design [antenna applications corner]," *IEEE Antennas Propag. Mag.*, vol. 62, no. 5, pp. 95–107, Oct. 2020.
[48] E. Kwiatkowski, J. A. Estrada, A. López-Yela, and Z. Popović, "Broadband RF energy-harvesting arrays," *Proc. IEEE*, vol. 110, no. 1, pp. 74–88, Jan. 2022.
[49] X. Gu, S. Hemour, and K. Wu, "Far-field wireless power harvesting: Nonlinear modeling, rectenna design, and emerging applications," *Proc. IEEE*, vol. 110, no. 1, pp. 56–73, Jan. 2022.
[50] C. R. Valenta and G. D. Durgin, "Harvesting wireless power: Survey of energy-harvester conversion efficiency in far-field, wireless power transfer systems," *IEEE Microw. Mag.*, vol. 15, no. 4, pp. 108–120, Jun. 2014.
[51] M. Wagih, A. S. Weddell, and S. Beeby, "Millimeter-wave power harvesting: A review," *IEEE Open J. Antennas Propag.*, vol. 1, pp. 560–578, 2020.
[52] K. Niotaki, A. Georgiadis, and A. Collado, "Dual-band rectifier based on resistance compression networks," in *Proc. IEEE MTT-S Int. Microw. Symp.*, 2014, pp. 1–3.
[53] T. W. Barton, J. M. Gordonson, and D. J. Perreault, "Transmission line resistance compression networks and applications to wireless power transfer," *IEEE Trans. Emerg. Sel. Topics Power Electron.*, vol. 3, no. 1, pp. 252–260, Mar. 2015.
[54] J. Liu, X. Y. Zhang, and Q. Xue, "Dual-band transmission-line resistance compression network and its application to rectifiers," *IEEE Trans. Circuits Syst. I, Reg. Papers*, vol. 66, no. 1, pp. 119–132, Jan. 2019.
[55] K. Niotaki, S. Kim, S. Jeong, A. Collado, A. Georgiadis, and M. M. Tentzeris, "A compact dual-band rectenna using slot-loaded dual band folded dipole antenna," *IEEE Antennas Wireless Propag. Lett.*, vol. 12, pp. 1634–1637, 2013.
[56] A. Collado and A. Georgiadis, "Conformal hybrid solar and electromagnetic (EM) energy harvesting rectenna," *IEEE Trans. Circuits Syst. I, Reg. Papers*, vol. 60, no. 8, pp. 2225–2234, Aug. 2013.
[57] X. Gu, L. Guo, S. Hemour, and K. Wu, "Optimum temperatures for enhanced power conversion efficiency (PCE) of zero-bias diode-based rectifiers," *IEEE Trans. Microw. Theory Techn.*, vol. 68, no. 9, pp. 4040–4053, Sep. 2020.
[58] H. C. Torrey and C. A. Whitmer, *Crystal Rectifiers*. New York, NY, USA: McGraw-Hill, 1948.
[59] S. Hemour et al., "Towards low-power high-efficiency RF and microwave energy harvesting," *IEEE Trans. Microw. Theory Techn.*, vol. 62, no. 4, pp. 965–976, Apr. 2014.
[60] N. Jin, R. Yu, S.-Y. Chung, P. Berger, P. Thompson, and P. Fay, "High sensitivity Si-based backward diodes for zero-biased square-law detection and the effect of post-growth annealing on performance," *IEEE Electron Device Lett.*, vol. 26, no. 8, pp. 575–578, Aug. 2005.
[61] C. H. P. Lorenz et al., "Breaking the efficiency barrier for ambient microwave power harvesting with heterojunction backward tunnel diodes," *IEEE Trans. Microw. Theory Techn.*, vol. 63, no. 12, pp. 4544–4555, Dec. 2015.
[62] Y. Zhang, S. Shen, C. Y. Chiu, and R. Murch, "Hybrid RF-solar energy harvesting systems utilizing transparent multiport micromeshed antennas," *IEEE Trans. Microw. Theory Techn.*, vol. 67, no. 11, pp. 4534–4546, Nov. 2019.
[63] M. Virili et al., "Performance improvement of rectifiers for WPT exploiting thermal energy harvesting," *Wireless Power Transfer*, vol. 2, no. 1, pp. 22–31, 2015.
[64] X. Gu, S. Hemour, L. Guo, and K. Wu, "Integrated cooperative ambient power harvester collecting ubiquitous radio frequency and kinetic energy," *IEEE Trans. Microw. Theory Techn.*, vol. 66, no. 9, pp. 4178–4190, Sep. 2018.
[65] G. De Vita and G. Iannaccone, "Design criteria for the RF section of UHF and microwave passive RFID transponders," *IEEE Trans. Microw. Theory Techn.*, vol. 53, no. 9, pp. 2978–2990, Sep. 2005.
[66] J. Kimionis, A. Collado, M. Tentzeris, and A. Georgiadis, "Octave and decade printed UWB rectifiers based on nonuniform transmission lines for energy harvesting," *IEEE Trans. Microw. Theory Techn.*, vol. 65, no. 11, pp. 4326–4334, Nov. 2017.
[67] R. M. Fano, "Theoretical limitations on the broadband matching of arbitrary impedances," Res. Lab. Electron., Massachusetts Inst. Technol., Cambridge, MA, USA, Tech. Rep. 41, Jan. 1948.
[68] S. Daskalakis, J. Kimionis, J. Hester, A. Collado, M. M. Tentzeris, and A. Georgiadis, "Inkjet printed 24 GHz rectenna on paper for millimeter wave identification and wireless power transfer applications," in *Proc. IEEE MTT-S Int. Microw. Workshop Ser. Adv. Mater. Processes RF THz Appl.*, 2017, pp. 1–3.
[69] M. Bozzi, A. Georgiadis, and K. Wu, "Review of substrate-integrated waveguide circuits and antennas," *IET Microw. Antennas Propag.*, vol. 5, no. 8, pp. 909–920, 2011.
[70] A. Collado and A. Georgiadis, "24 GHz substrate integrated waveguide (SIW) rectenna for energy harvesting and wireless power transmission," in *Proc. IEEE MTT-S Int. Microw. Symp.*, 2013, pp. 1–3.
[71] M. Shanawani, D. Masotti, and A. Costanzo, "THz rectennas and their design rules," *Electronics*, vol. 6, no. 4, 2017, Art. no. 99. [Online]. Available: https://www.mdpi.com/2079-9292/6/4/99
[72] C. Song, J. Zhou, J. Zhang, S. Yuan, and P. Carter, "A high-efficiency broadband rectenna for ambient wireless energy harvesting," *IEEE Trans. Antennas Propag.*, vol. 63, no. 8, pp. 3486–3495, Aug. 2015.
[73] C. Song et al., "A novel six-band dual CP rectenna using improved impedance matching technique for ambient RF energy harvesting," *IEEE Trans. Antennas Propag.*, vol. 64, no. 7, pp. 3160–3171, Jul. 2016.
[74] F. Bolos, J. Blanco, A. Collado, and A. Georgiadis, "RF energy harvesting from multi-tone and digitally modulated signals," *IEEE Trans. Microw. Theory Techn.*, vol. 64, no. 6, pp. 1918–1927, Jun. 2016.
[75] A. Collado et al., "Rectifier design challenges for RF wireless power transfer and energy harvesting systems," *Radioengineering*, vol. 26, no. 2, pp. 411–417, 2017.
[76] X. Gu, S. Hemour, and K. Wu, "Wireless powered sensors for battery-free IoT through multi-stage rectifier," in *Proc. 33rd Gen. Assem. Sci. Symp. Int. Union Radio Sci.*, 2020, pp. 1–4.
[77] J. Finnegan, K. Niotaki, and S. Brown, "Exploring the boundaries of ambient RF energy harvesting with LoRaWAN," *IEEE Internet Things J.*, vol. 8, no. 7, pp. 5736–5743, Apr. 2021.
[78] K. Gumber, C. Dejous, and S. Hemour, "Harmonic reflection amplifier for widespreadbackscatter Internet-of-Things," *IEEE Trans. Microw. Theory Techn.*, vol. 69, no. 1, pp. 774–785, Jan. 2021.
[79] S. Assimonis, V. Fusco, and A. Georgiadis, "Efficient and sensitive electrically small rectenna for ultra-low power RF energy harvesting," *Sci. Rep.*, vol. 8, no. 1, pp. 1–13, 2018.
[80] J.-J. Lu, X.-X. Yang, H. Mei, and C. Tan, "A four-band rectifier with adaptive power for electromagnetic energy harvesting," *IEEE Microw. Wireless Compon. Lett.*, vol. 26, no. 10, pp. 819–821, Oct. 2016.
[81] V. Kuhn, C. Lahuec, F. Seguin, and C. Person, "A multi-band stacked RF energy harvester with RF-to-DC efficiency up to 84%," *IEEE Trans. Microw. Theory Techn.*, vol. 63, no. 5, pp. 1768–1778, May 2015.
[82] D. Khan et al., "A design of ambient RF energy harvester with sensitivity of −21 dBm and power efficiency of a 39.3 % using internal threshold voltage compensation," *Energies*, vol. 11, no. 5, 2018, Art. no. 1258. [Online]. Available: https://www.mdpi.com/1996-1073/11/5/1258
[83] S. M. Noghabaei, R. L. Radin, Y. Savaria, and M. Sawan, "A high-efficiency ultra-low-power CMOS rectifier for RF energy harvesting applications," in *Proc. IEEE Int. Symp. Circuits Syst.*, 2018, pp. 1–4.

[84] T. J. Lee et al., "Design of efficient rectifier for low-power wireless energy harvesting at 2.45 Ghz," in *Proc. IEEE Radio Wireless Symp.*, 2015, pp. 47–49.

[85] H. Zhang, Y.-X. Guo, Z. Zhong, and W. Wu, "Cooperative integration of RF energy harvesting and dedicated WPT for wireless sensor networks," *IEEE Microw. Wireless Compon. Lett.*, vol. 29, no. 4, pp. 291–293, Apr. 2019.

[86] S.-E. Adami et al., "A flexible 2.45-GHz power harvesting wristband with net system output from −24.3 dBm of RF power," *IEEE Trans. Microw. Theory Techn.*, vol. 66, no. 1, pp. 380–395, Jan. 2018.

[87] U. Olgun, C.-C. Chen, and J. L. Volakis, "Investigation of rectenna array configurations for enhanced RF power harvesting," *IEEE Antennas Wireless Propag. Lett.*, vol. 10, pp. 262–265, 2011.

[88] H. Sun, Y.-x. Guo, M. He, and Z. Zhong, "Design of a high-efficiency 2.45-GHz rectenna for low-input-power energy harvesting," *IEEE Antennas Wireless Propag. Lett.*, vol. 11, pp. 929–932, 2012.

[89] J. Costantine, A. Eid, M. Abdallah, Y. Tawk, and A. H. Ramadan, "A load independent tapered RF harvester," *IEEE Microw. Wireless Compon. Lett.*, vol. 27, no. 10, pp. 933–935, Oct. 2017.

[90] C.-H. Chin, Q. Xue, and C. H. Chan, "Design of a 5.8-GHz rectenna incorporating a new patch antenna," *IEEE Antennas Wireless Propag. Lett.*, vol. 4, pp. 175–178, 2005.

[91] K. Nishida et al., "5.8 GHz high sensitivity rectenna array," in *Proc. IEEE MTT-S Int. Microw. Workshop Ser. Innov. Wireless Power Transmiss.: Technol., Syst., Appl.*, 2011, pp. 19–22.

[92] D. Wang and R. Negra, "Design of a dual-band rectifier for wireless power transmission," in *Proc. IEEE Wireless Power Transfer*, 2013, pp. 127–130.

[93] K. Hamano, A. Suzuki, K. Nishikawa, and S. Kawasaki, "2.4/5.8GHz dual-band rectifiers for aerospace wireless sensor and RF energy harvester system," in *Proc. IEEE Radio Wireless Symp.*, 2019, pp. 1–4.

[94] S. Dehghani, S. Mirabbasi, and T. Johnson, "A 5.8-GHz bidirectional and reconfigurable RF energy harvesting circuit with rectifier and oscillator modes," *IEEE Solid-State Circuits Lett.*, vol. 1, no. 3, pp. 66–69, Mar. 2018.

[95] S. Ladan, A. B. Guntupalli, and K. Wu, "A high-efficiency 24 GHz rectenna development towards millimeter-wave energy harvesting and wireless power transmission," *IEEE Trans. Circuits Syst. I, Reg. Papers*, vol. 61, no. 12, pp. 3358–3366, Dec. 2014.

[96] P. Burasa, N. G. Constantin, and K. Wu, "High-efficiency wideband rectifier for single-chip batteryless active millimeter-wave identification (MMID) tag in 65-nm bulk CMOS technology," *IEEE Trans. Microw. Theory Techn.*, vol. 62, no. 4, pp. 1005–1011, Apr. 2014.

[97] A. Riaz, S. Zakir, M. M. Farooq, M. Awais, and W. T. Khan, "A triband rectifier toward millimeter-wave frequencies for energy harvesting and wireless power-transfer applications," *IEEE Microw. Wireless Compon. Lett.*, vol. 31, no. 2, pp. 192–195, Feb. 2021.

[98] D. Matos, R. Correia, and N. B. Carvalho, "Millimeter-wave hybrid RF-DC converter based on a GaAs chip for IoT-WPT applications," *IEEE Microw. Wireless Compon. Lett.*, vol. 31, no. 6, pp. 787–790, Jun. 2021.

[99] A. Riaz, M. Awais, M. M. Farooq, and W. T. Khan, "A single cell dual band rectifier at millimeter-wave frequencies for future 5G communications," in *Proc. 49th Eur. Microw. Conf.*, 2019, pp. 41–44.

[100] S. Ladan and K. Wu, "Nonlinear modeling and harmonic recycling of millimeter-wave rectifier circuit," *IEEE Trans. Microw. Theory Techn.*, vol. 63, no. 3, pp. 937–944, Mar. 2015.

[101] P. He and D. Zhao, "High-efficiency millimeter-wave CMOS switching rectifiers: Theory and implementation," *IEEE Trans. Microw. Theory Techn.*, vol. 67, no. 12, pp. 5171–5180, Dec. 2019.

[102] Y. Wang, X.-X. Yang, G.-N. Tan, and S. Gao, "Study on millimeter-wave SIW rectenna and arrays with high conversion efficiency," *IEEE Trans. Antennas Propag.*, vol. 69, no. 9, pp. 5503–5511, Sep. 2021.

[103] H. Gao et al., "A 71 GHz RF energy harvesting tag with 8 efficiency for wireless temperature sensors in 65 nm CMOS," in *Proc. IEEE Radio Freq. Integr. Circuits Symp.*, 2013, pp. 403–406.

[104] S. Hemour, C. H. P. Lorenz, and K. Wu, "Small-footprint wideband 94Hhz rectifier for swarm micro-robotics," in *Proc. IEEE MTT-S Int. Microw. Symp.*, 2015, pp. 1–4.

[105] K. Matsui et al., "Microstrip antenna and rectifier for wireless power transfar at 94 GHz," in *Proc. IEEE Wireless Power Transfer Conf.*, 2017, pp. 1–3.

[106] K. Matsui, K. Komurasaki, W. Hatakeyama, K. Shimamura, K. Fujiwara, and H. Yamaoka, "Development of a 100 mW-class 94 GHz high-efficiency single-series rectifier feed by finline for micro-UAV application," *Proc. Act. Passive Electron. Compon.*, vol. 2020, 2020.

[107] H. Kazemi, "61.5% efficiency and 3.6 kw/m2 power handling rectenna circuit demonstration for radiative millimeter wave wireless power transmission," *IEEE Trans. Microw. Theory Techn.*, vol. 70, no. 1, pp. 650–658, Jan. 2022.

[108] E. Shaulov, S. Jameson, and E. Socher, "W-band energy harvesting rectenna array in 65-nm CMOS," in *Proc. IEEE MTT-S Int. Microw. Symp.*, 2017, pp. 307–310.

[109] P. Zhu, Z. Ma, G. A. E. Vandenbosch, and G. Gielen, "160 GHz harmonic-rejecting antenna with CMOS rectifier for millimeter-wave wireless power transmission," in *Proc. 9th Eur. Conf. Antennas Propag.*, 2015, pp. 1–5.

[110] M. I. W. Khan, E. Lee, N. M. Monroe, A. P. Chandrakasan, and R. Han, "A dual-antenna, 263-GHz energy harvester in CMOS for ultra-miniaturized platforms with 13.6% RF-to-DC conversion efficiency at 8 dBm input power," in *Proc. IEEE Radio Freq. Integr. Circuits Symp.*, 2022, pp. 291–294.

[111] S. Mizojiri et al., "Subterahertz wireless power transmission using 303-GHz rectenna and 300-kW-class Gyrotron," *IEEE Microw. Wireless Compon. Lett.*, vol. 28, no. 9, pp. 834–836, Sep. 2018.

[112] X. Gu, N.N. Srinaga, L. Guo, S. Hemour, and K. Wu, "Diplexer-based fully passive harmonic transponder for Sub-6-GHz 5G-Compatible IoT applications," *IEEE Trans. Microw. Theory Techn.*, vol. 67, no. 5, pp. 1675–1687, May 2019.

[113] X. Gu, W. Lin, S. Hemour, and K. Wu, "Readout distance enhancement of battery-free harmonic transponder," *IEEE Trans. Microw. Theory Techn.*, vol. 69, no. 7, pp. 3413–3424, Jul. 2021.

[114] J.-G. J. Zhu and C. Park, "Magnetic tunnel junctions," *Mater. Today*, vol. 9, no. 11, pp. 36–45, Nov. 2006.

[115] S. Muhammad, J. J. Tiang, S. K. Wong, A. Smida, R. Ghayoula, and A. Iqbal, "A dual-band ambient energy harvesting rectenna design for wireless power communications," *IEEE Access*, vol. 9, pp. 99944–99953, 2021.

[116] H. Tafekirt, J. Pelegri-Sebastia, A. Bouajaj, and B. M. Reda, "A sensitive triple-band rectifier for energy harvesting applications," *IEEE Access*, vol. 8, pp. 73659–73664, 2020.

[117] A. Costanzo, F. Benassi, and G. Monti, "Wearable, energy-autonomous RF microwave systems: Chipless and energy-harvesting-based wireless systems for low-power, low-cost localization and sensing," *IEEE Microw. Mag.*, vol. 23, no. 3, pp. 24–38, Mar. 2022.

[118] V. Palazzi, S. Bonafoni, F. Alimenti, P. Mezzanotte, and L. Roselli, "Feeding the world with microwaves: How remote and wireless sensing can help precision agriculture," *IEEE Microw. Mag.*, vol. 20, no. 12, pp. 72–86, Dec. 2019.

[119] V. Palazzi et al., "Radiative wireless power transfer: Where we are and where we want to go," *IEEE Microw. Mag.*, vol. 24, no. 2, pp. 57–79, Feb. 2023.

[120] C. Song, P. Lu, and S. Shen, "Highly efficient omnidirectional integrated multiband wireless energy harvesters for compact sensor nodes of Internet-of-Things," *IEEE Trans. Ind. Electron.*, vol. 68, no. 9, pp. 8128–8140, Sep. 2021.

[121] M. Wagih, A. S. Weddell, and S. Beeby, "Omnidirectional dual-polarized low-profile textile rectenna with over 50% Efficiency for Sub-μW/cm^2 wearable power harvesting," *IEEE Trans. Antennas Propag.*, vol. 69, no. 5, pp. 2522–2536, May 2021.

[122] V. Palazzi et al., "Performance analysis of a ultra-compact low-power rectenna in paper substrate for RF energy harvesting," in *Proc. IEEE Topical Conf. Wireless Sensors Sensor Netw.*, 2017, pp. 65–68.

[123] S. Bandyopadhyay, P. P. Mercier, A. C. Lysaght, K. M. Stankovic, and A. P. Chandrakasan, "A 1.1 nW energy-harvesting system with 544 pW quiescent power for next-generation implants," *IEEE J. Solid-State Circuits*, vol. 49, no. 12, pp. 2812–2824, Dec. 2014.

[124] V. Palazzi et al., "A novel ultra-lightweight multiband rectenna on paper for RF energy harvesting in the next generation LTE bands," *IEEE Trans. Microw. Theory Techn.*, vol. 66, no. 1, pp. 366–379, Jan. 2018.

[125] M. Wagih, G. S. Hilton, A. S. Weddell, and S. Beeby, "Broadband millimeter-wave textile-based flexible rectenna for wearable energy harvesting," *IEEE Trans. Microw. Theory Techn.*, vol. 68, no. 11, pp. 4960–4972, Nov. 2020.

[126] J. Bito et al., "Millimeter-wave ink-jet printed RF energy harvester for next generation flexible electronics," in *Proc. IEEE Wireless Power Transfer Conf.*, 2017, pp. 1–4.

[127] J. Hagerty, F. Helmbrecht, W. McCalpin, R. Zane, and Z. Popovic, "Recycling ambient microwave energy with broad-band rectenna arrays," *IEEE Trans. Microw. Theory Techn.*, vol. 52, no. 3, pp. 1014–1024, Mar. 2004.

[128] M. Wagih and S. Beeby, "Thin flexible RF energy harvesting rectenna surface with a large effective aperture for sub μW/cm^2 powering of wireless sensor nodes," *IEEE Trans. Microw. Theory Techn.*, vol. 70, no. 9, pp. 4328–4338, Sep. 2022.

[129] C. Kalialakis and A. Georgiadis, "The regulatory framework for wireless power transfer systems," *Wireless Power Transfer*, vol. 1, no. 2, pp. 108–118, 2014.

[130] M. Xia and S. Aissa, "On the efficiency of far-field wireless power transfer," *IEEE Trans. Signal Process.*, vol. 63, no. 11, pp. 2835–2847, Jun. 2015.

[131] R. A. M. Pereira and N. B. Carvalho, "Quasioptics for increasing the beam efficiency of wireless power transfer systems," *Sci. Rep.*, vol. 12, no. 1, 2022, Art. no. 20894.

[132] R. A. M. Pereira and N. B. Carvalho, "Quasioptical dielectric lens system for WPT solutions," in *Proc. Wireless Power Week*, 2022, pp. 190–194.

[133] T. Takano, T. Uno, K. Shibata, and K. Saegusa, "Generation of a beamed wave using a phased array antenna," in *Proc. URSI Asia-Pacific Radio Sci. Conf.*, 2016, pp. 377–379.

[134] K. Niotaki, M. J. Cañavate-Sánchez, A. Collado, G. Goussetis, A. Georgiadis, and T. Brazil, "2.45 GHz/5.8 GHz dual-band power amplifier for wireless power transfer in space applications," in *Proc. Act. Passive RF Devices* 2017, pp. 1–4.

[135] Y. Karandikar, "Factorization of Gaussian coupling efficiency and algorithm to compute it," in *Proc. 6th Eur. Conf. Antennas Propag.*, 2012, pp. 868–872.

[136] P. Goldsmith, *Quasioptical Systems: Gaussian Beam Quasioptical Propagation and Applications*. Piscataway, NJ, USA: IEEE Press, 1998.

[137] Y. T. Lo and S. W. Lee, *Antenna Handbook: Volume II Antenna Theory*. Van Nostrand Reinhold, New York, NY: Springer, 1993.

[138] C. H. P. Lorenz, S. Hemour, and K. Wu, "Physical mechanism and theoretical foundation of ambient RF power harvesting using zero-bias diodes," *IEEE Trans. Microw. Theory Techn.*, vol. 64, no. 7, pp. 2146–2158, Jul. 2016.

[139] J. Kang, P. Chiang, and A. Natarajan, "A 3.6 cm^2 wirelessly-powered UWB SoC with -30.7 dBm rectifier sensitivity and sub-10 cm range resolution," in *Proc. IEEE Radio Freq. Integr. Circuits Symp.*, 2015, pp. 255–258.

[140] T. Bjorninen, L. Ukkonen, and Y. Rahmat-Samii, "Advances in antenna designs for UHF RFID tags mountable on conductive items," *IEEE Antennas Propag. Mag.*, vol. 56, no. 1, pp. 79–103, Feb. 2014.

[141] A. Eid, J. Hester, and M. Tentzeris, "5G as a wireless power grid," *Nature Sci. Rep.*, vol. 11, no. 1, pp. 1–9, 2021.

[142] A. Eid, J. Hester, B. Tehrani, and M. Tentzeris, "flexible W-band rectifiers for 5G-powered IoT autonomous modules," in *Proc. IEEE Int. Symp. Antennas Propag. USNC-URSI Radio Sci. Meeting*, Atlanta, GA, USA, 2019, pp. 1163–1164.

[143] H. Gao, M. K. Matters-Kammerer, D. Milosevic, A. V. Roermund, and P. Baltus, "A 50–60 GHz rectifier with -7 dBm sensitivity for 1 V DC output voltage and 8% efficiency in 65-nm CMOS," in *Proc. IEEE MTT-S Int. Microw. Symp.*, 2014, pp. 1–3.

[144] N. Weissman, S. Jameson, and E. Socher, "W-band CMOS on-chip energy harvester and rectenna," in *Proc. IEEE MTT-S Int. Microw. Symp.*, 2014, pp. 1–3.

[145] W. Rotman and R. Turner, "Wide-angle microwave lens for line source applications," *IEEE Trans. Antennas Propag.*, vol. 11, no. 6, pp. 623–632, Nov. 1963.

[146] A. Eid, J. G. Hester, and M. M. Tentzeris, "Rotman lens-based wide angular coverage and high-gain semipassive architecture for ultra-long range mm-wave RFIDs," *IEEE Antennas Wireless Propag. Lett.*, vol. 19, no. 11, pp. 1943–1947, Nov. 2020.

[147] A. Eid, J. Hester, and M. M. Tentzeris, "A scalable high-gain and large-beamwidth mm-wave harvesting approach for 5G-powered IoT," in *Proc. IEEE MTT-S Int. Microw. Symp.*, 2019, pp. 1309–1312.

[148] E. Vandelle, H. Bui, T.-P. Vuong, G. Ardilla, K. Wu, and S. Hemour, "Harvesting ambient RF energy efficiently with optimal angular coverage," *IEEE Trans. Antennas Propag.*, vol. 67, no. 3, pp. 1862–1873, Mar. 2019.

[149] B. Marshall, C. Valenta, and G. D. Durgin, "DC power pattern analysis of n-by-n staggered pattern charge collector and n2 rectenna array,," in *Proc. IEEE Wireless Power Transfer*, 2013, pp. 115–118.

[150] A. Eid, J. Hester, and M. M. Tentzeris, "Extending the range of 5G energy transfer: Towards the wireless power grid," in *Proc. 16th Eur. Conf. Antennas Propag.*, Madrid, Spain, 2022, pp. 1–4.

[151] P. Pusula et al., "Millimeter-wave identification—A new short-range radio system for low-power high data-rate applications," *IEEE Trans. Microw. Theory Techn.*, vol. 56, no. 10, pp. 2221–2228, Oct. 2008.

[152] J. G. Hester and M. M. Tentzeris, "Inkjet-printed flexible mm-wave Van-Atta reflectarrays: A solution for ultralong-range dense multitag and multisensing chipless RFID implementations for IoT smart skins," *IEEE Trans. Microw. Theory Techn.*, vol. 64, no. 12, pp. 4763–4773, Dec. 2016.

[153] J. Hester and M. Tentzeris, "Inkjet-printed van-atta reflectarray sensors: A new paradigm for long-range chipless low cost ubiquitous smart skin sensors of the Internet of Things," in *Proc. IEEE MTT-S Int. Microw. Symp.*, 2016, pp. 1–4.

[154] A. Pacini, A. Costanzo, S. Aldhaher, and P. D. Mitcheson, "Load- and position-independent moving MHz WPT system based on GaN-distributed current sources," *IEEE Trans. Microw. Theory Techn.*, vol. 65, no. 12, pp. 5367–5376, Dec. 2017.

[155] A. Pacini, F. Berra, D. Masotti, and A. Costanzo, "Uniform sliding system for simultaneous WPT and communication data transfer," in *Proc. IEEE Radio Wireless Symp.*, 2019, pp. 1–3.

[156] R. Trevisan and A. Costanzo, "A UHF near-field link for passive sensing in industrial wireless power transfer systems," *IEEE Trans. Microw. Theory Techn.*, vol. 64, no. 5, pp. 1634–1643, May 2016.

[157] N. Decarli, M. D. Prete, D. Masotti, D. Dardari, and A. Costanzo, "High-accuracy localization of passive tags with multisine excitations," *IEEE Trans. Microw. Theory Techn.*, vol. 66, no. 12, pp. 5894–5908, Dec. 2018.

[158] M. Wagih, G. S. Hilton, A. S. Weddell, and S. Beeby, "Dual-band dual-mode textile antenna/rectenna for simultaneous wireless information and power transfer (SWIPT)," *IEEE Trans. Antennas Propag.*, vol. 69, no. 10, pp. 6322–6332, Oct. 2021.

[159] P. Lu, C. Song, and K. M. Huang, "A two-port multipolarization rectenna with orthogonal hybrid coupler for simultaneous wireless information and power transfer (SWIPT)," *IEEE Trans. Antennas Propag.*, vol. 68, no. 10, pp. 6893–6905, Oct. 2020.

[160] H. Zhang, Y. Li, S.-P. Gao, and Y.-X. Guo, "High-efficiency simultaneous wireless information and power transmission (SWIPT) by exploiting 2nd/3rd harmonics," in *Proc. IEEE MTT-S Int. Wireless Symp.*, 2021, pp. 1–3.

[161] G. Paolini, A. Quddious, D. Chatzichristodoulou, D. Masotti, S. Nikolaou, and A. Costanzo, "An energy-autonomous swipt rfid tag for communication in the 2.4 GHz ISM band," in *Proc. 3rd URSI Atlantic Asia Pacific Radio Sci. Meeting*, 2022, pp. 1–4.

[162] M. Rajabi, N. Pan, S. Claessens, S. Pollin, and D. Schreurs, "Modulation techniques for simultaneous wireless information and power transfer with an integrated rectifier–receiver," *IEEE Trans. Microw. Theory Techn.*, vol. 66, no. 5, pp. 2373–2385, May 2018.